EFFECT OF FSP ON SPRAY FORMED Al-Si ALLOY

A

Dissertation

submitted in partial fulfilment of the requirements for the degree

of

Masters of Technology

in

DEPARTMENT OF METALLURGICAL AND MATERIALS ENGINEERING

(With specialization in Materials Engineering)

By

Abhijeet Bajpai

(14545001)

Under Supervision of:

Dr. Devendra Singh

Department of Metallurgical and Materials Engineering

Indian Institute of Technology, Roorkee

Year: 2016

EFFECT OF FSP ON SPRAY FORMED Al-Si ALLOY

A

Dissertation

submitted in partial fulfilment of the requirements for the Degree

of

Masters of Technology

in

METALLURGICAL AND MATERIALS ENGINEERING

(With specialization in Materials Engineering)

By

Abhijeet Bajpai

(14545001)

Under supervision of:

Dr. Devendra Singh

Department of Metallurgical and Materials Engineering

Indian Institute of Technology, Roorkee

Year: 2016

CANDIDATE'S DECLARATION

I hereby declare that the work, which is being presented in this dissertation entitled "**Effect of FSP on the Spray formed Al-Si alloy**" in partial fulfilment of the requirements for the award of the degree of **Master of Technology** in the metallurgical and materials engineering with specialization in "**Materials Engineering**" submitted in Department of **Metallurgical and Materials Engineering,** Indian Institute of Technology, Roorkee, India, is an authentic record of our own work carried during the period from June 2015 to June 2016 under the supervision and guidance of Dr. Devendra Singh, Associate Professor, Department of Metallurgical and Materials Engineering, Indian Institute of Technology, Roorkee (India).

I have not submitted the matter embodied in this dissertation for the award of any other degree.

Dated: June 2016 _____

Place: IIT, Roorkee Abhijeet Bajpai

14545001

CERTIFICATE

This is to certify that the above statement made by the candidate is correct to the best of my knowledge.

Dr. Devendra Singh

Associate Professor

Department of Metallurgical and Materials Engineering

Indian Institute of Technology, Roorkee

Roorkee-247667(India)

ACKNOWLEDGMENT

I am deeply indebted to my guide Dr. Devendra Singh, Associate Professor, Department of Metallurgical and Materials Engineering, Indian Institute of Technology, Roorkee for encouraging me to undertake this project as well as providing me all necessary guidance and inspirational support throughout this dissertation work. He has displayed unique tolerance and understanding at every step of progress. It is my proud privilege to have carried out this dissertation work under his able guidance.

I am highly thankful to Dr. Anjan Sil, Professor and Head, Department of Metallurgical and Materials engineering, India Institute of Technology, Roorkee, for providing me all necessary facilities in the department to complete this work.

I would like to thank to all my teachers here in the department of Metallurgical and Materials engineering who made me capable of doing all this work. I am also thankful to the staff members of fabrication lab, metallography lab, material testing lab and tribology lab who helped me whole heartedly.

I do not have enough words to thank all my seniors who encouraged and helped me to complete this work. Also, I would like to thank my seniors Aniruddha Malakar, Surendra Kumar Chourasiya and Sandeep Kumar whose constant support and guidance helped me throughout the work.

I'm also thankful to my batch mates who encouraged and helped me to complete this work. Also, I would like to thank my classmates Supratim Endow, Niranjan Kumar and Yogendra Pratap Singh for their constant help throughout the work.

Abhijeet Bajpai

14545001

ABSTRACT

Spray Forming (SF) is an advanced materials processing technology that transforms molten metal into a near-net-shape solid by depositing atomized droplets onto a substrate. As Aluminum (Al) – Silicon (Si) alloy with addition of graphite provides for low weight, low cost and high performance in structural materials [3]. Processing of these composites by the conventional casting routes is difficult due to liquid immiscibility and floating of low-density graphite(Gr) powder during melt solidification. In the present investigation, Al-Si-Gr composite is produced by spray forming and then friction stir processing (FSP) was introduced to refine the microstructure of spray formed Al-Si-Gr composite. The aim of the current research work is to study the Al-Si alloy with addition of graphite and examine the changes produced in microstructure and mechanical properties of the material after FSP. In this study, Al-Si-Gr composites for cylinder liner application were synthesized using spray forming technique, aiming on improving its wear resistance. Silicon (Si) and graphite (Gr) particles, which do not get distributed uniformly in Al-matrix by conventional processes, are distributed uniformly throughout the casting using spray forming. Disc shape spray deposit castings were made of Al–6Si-5Gr, Al-12Si-5Gr and Al–18Si-5Gr composite, and then their microstructures were studied. In spray form castings, it was found that the Si particles were distributed homogeneously in the Al-matrix. In addition to that, spray formed Al-Si-Gr composites were subjected to the friction stir processing (FSP). FSP was introduced to eliminate the porosity present in the spray formed composite and also for further refinement of microstructure of spray formed Al-Si-Gr composite. Microstructure of stir zone (SZ) was observed to be highly refined compared to the spray formed material. FSP resulted in complete homogenization and elimination of casting defects especially porosity. Mechanical properties like hardness and tensile strength were sharply improved after FSP.

TABLE OF CONTENTS

Page No.

List of Acronyms and Abbreviations

Advancing side	AS
Aluminium	Al
Dynamically Recrystallized Zone	DRZ
Figure	Fig.
Friction Stir Processing	FSP
Friction Stir Welding	FSW
Horse Power	HP
Kilogram force	kgf
Magnesium Oxide	MgO
Mega Pascal	MPa
Melting Point	MP
Mild Steel	MS
Scanning Electron Microscope	SEM
Spray Forming	SF
Stir Zone	SZ
Rotations per minute	rpm
Ultimate Tensile Strength	UTS

List of Symbols

G	Matrix shear modulus
b	Burgers vector
ν	Poisson's ratio
$\mathbf{r_0}$	Dislocation core radius
λ	Inter-particle spacing
E_2	Young's moduli of the composite
E_m	Young's moduli of the matrix
E_f	Young's moduli of the reinforcement
ξ	Adjustable parameter
f	Volume fraction of the particles.

List of Figures

List of Tables

CHAPTER 1
INTRODUCTION

Spray deposition is a method of casting metal components with cellular, fine-grained, equi-axed and homogeneous microstructure. Which are beyond the reach of conventional casting technique, via the deposition of semi-solid sprayed droplets on to a substrate. The resulting part exhibits a rapidly solidified microstructure with highly refined grain size and reduced levels of segregation. However, a spray formed material is generally porous with poor mechanical properties [11]. To prepare fully dense metal with high mechanical properties, the porous preform must further be densified and deformed plastically. Effective methods like Forging, extrusion, rolling, etc. are conventionally used to eliminate porosity of the preform and also to achieve required mechanical properties like hardness, tensile strength and wear resistance [12].

The mixing of graphite in Al-Si alloys is very difficult through conventional casting routes because of high density difference and melting point (MT) difference between graphite and aluminium-silicon alloy. The effective methods used to densify the material as well as to achieve the required mechanical properties are rolling, forging, hot pressing, extrusion etc. but recently friction stir processing (FSP) was developed by Mishra et al. as a comprehensive tool for microstructural modification based on the basic principles of friction stir welding (FSW). In this processing, a rotating tool generally made of die-steel is inserted in a monolithic work piece like Al alloys for confined microstructural modification for specific property enhancement. FSP diminishes the pores present in work-piece and refines the microstructure [46]. The most significant objective of FSP in spray deposited material is to minimize porosity [13]. We need strength and anti-wear properties in cylindrical linings with a good surface for the piston rings to slide along its length. Cast Iron is the most widely used material mainly because of its good lubricating properties which is a result of graphite present in its micro-structure. Little porosity present in finally produced Al-Si-Gr composite can be useful as it would help to prevent or minimize the risk of seizure of the piston during its operation and also its a remedial measure against high galling (rubbing painfully; chafing) which takes place during piston movement. Cylinder liners can be directly made by spray casting as it produces near net shape. Aluminium based alloys have the advantage of high strength to weight ratio [26]. For cylinder linings application, the composites based on Al–Si-Gr system are potential materials because they have superior properties like better frictional properties, high thermal

conductivity, low weight and high performance without compromising with the strength and anti-corrosion property. Al-Si alloys also provide good surface finish [2].

Aluminium–Silicon alloys possess high strength to weight ratio, low thermal expansion coefficient and high wear resistance [27]. These alloys also show improved strength and wear properties as the silicon content is increased above eutectic composition. This is why this material is apt and suitable for our cylinder liners application purposes. Silicon imparts high fluidity and low shrinkage, which results in good cast ability and weld ability.

As solid lubricants are better than their liquid or semi-solid counterparts because they provide better properties during starting and warming up conditions [23]. Spray forming is good technique to disperse solid lubricant like graphite in Al-matrix to provide good anti-seizure and anti-frictional properties in cylindrical lining.

In the present research work spray forming was done to produce Al-Si-Gr composites of different concentrations and their microstructural and mechanical properties were studied. Due to high porosity present in spray deposited composites and their poor mechanical properties, we've performed FSP on the spray deposited composite. FSP not only reduced its porosity but also enhanced its mechanical properties with refinement in microstructure.

CHAPTER 2
LITERATURE REVIEW

2. 1 SPRAY FORMING

Spray deposition is a method of casting metal components with homogeneous microstructure which are beyond the reach of conventional casting technique, via the deposition of semi-solid droplets sprayed on to a substrate. Spray forming, also called spray casting or spray deposition, is the inert gas atomization of a liquid metal stream into variously sized droplets which are then propelled away from the region of atomization by the fast flowing, atomizing gas. The droplet trajectories are interrupted by a substrate which collects and solidifies the droplets into a coherent, near fully dense preform. This method has many advantages over conventional techniques like casting, powder metallurgy etc. In one particular method of spray forming, a steam of molten metal falling freely under gravity is atomized by a system of high pressure jets to form the required plume or spray droplets which, when they impinge on the suitably shaped receptor under appropriate conditions build up to form artefact for subsequent hot compaction as required [11]. It is a single step process, which produces near net shape so the cost of final product composite formed is less than the composites formed from other routes like powder metallurgy and direct chill casting [21]. Spray forming provides with improved elevated temperature strength coupled with good wear resistance in comparison to conventionally cast alloys [22]. There are various advantages provided by spray forming like fine scale microstructure, improved workability, less numbers of steps required, flexibility and near net shape formation. Spray forming is also an easy method to produce metal matrix composites compared to other routes [11,12,19]. There are various parameters which effect the properties of spray deposited material. These parameters are categorized into two parts. They are design parameters and operating parameters. Design parameters are design of atomizer, design of nozzle, throat diameter of nozzle, apex angle and width of nozzle's slit [17,18]. Operating parameters are pressure of the atomizing gas, gas type, alloy type and melt composition. We're using gas atomization with close coupled atomization, the gas atomizes the metal directly on exit from the melt delivery nozzle. We use gas atomization because aluminium has low melting. Atomized droplets of Al-Si alloy follow the Gaussian mass distribution about the cone axis of spray deposit [12,15].

Fig. 2.1 Photograph of spray forming setup

2.1.1 HISTORY OF SPRAY FORMING

Professor Singer at the Swansea University first developed the idea of gas atomised spray forming in the 1970s in which a high pressure gas jet impinges on a stable melt stream to cause atomisation. The resulting droplets are then collected on a target, which can be manipulated within the spray and used to form a near-dense billet of near-net shape. Spray forming has found applications in specialist industries such as: stainless steel cladding of incinerator tubes; nickel super alloy discs and rings for aerospace-engines; aluminium-titanium, aluminium-neodymium and aluminium-silver sputter targets; aluminium-silicon alloys for cylinder liners; and high speed steels. The history of spray forming of how spray forming then developed is an example of how the creative contributions of many researchers were necessary over a number of years to produce the innovation of a now widely used industrial process[28].

2.1.2 MICROSTRUCTURAL FEATURES

The balance between the heat input and heat output and the subsequent heat flow control the evolution of the spray formed microstructure [19]. Fine equiaxed grain morphology with a uniform distribution of Si phase in an Al-matrix. Silicon is present within the grains and along the grain boundary [6].

Srivastava et al. [8] have investigated the microstructural characteristics and mechanical properties of spray deposited Al-Si alloys. The results invariably exhibited considerable microstructural refinement in spray deposited Al-6.5Si and Al-18Si alloys. The resulting part exhibits a rapidly solidified microstructure with very refined grain sizes and reduced levels of segregation. The primary α phase in Al-6.5Si alloy revealed spherical morphology in contrast to its dendritic morphology in the as cast alloy. The size of the primary Si phase varied from 3 to 7 μm in the spray deposited Al-18Si alloy against their size of 100-130 μm in the as cast alloy.

Anand et al. [7] spray deposited Al-Si alloy. They observed that the microstructure of a conventional ingot metallurgy processed alloy exhibited coarse Si particulates, of varying size, distributed randomly through the microstructure whereas the spray deposited alloy revealed fine particulate shaped Si dispersoids distributed uniformly through the microstructure and equi-axed shaped grains.

Underhill et al. [49] have found that Spray-formed billet microstructures are controlled by the relationship between (1) the rate of heat input into the billet top surface, determined by the deposition rate and heat content of the arriving droplet spray, and (2) the rate of heat output from the billet top surface, determined by the extent of convective cooling into the gas and conductive cooling into the underlying billet and collector plate.

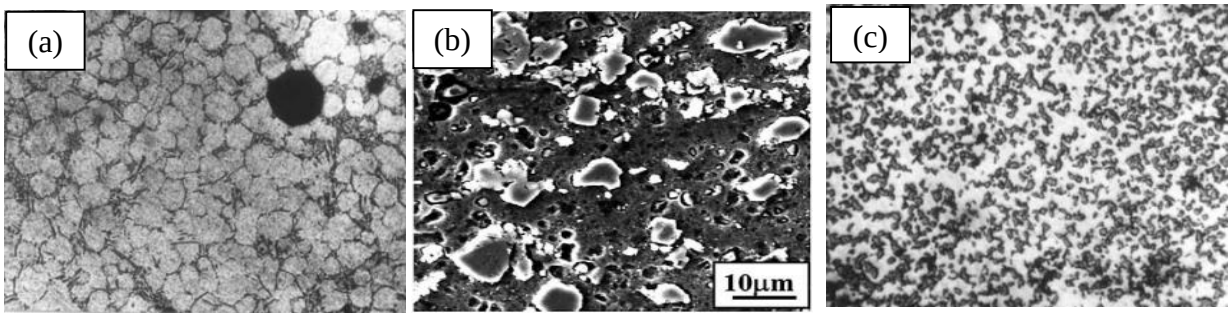

Fig. 2.2 Microstructure of Spray formed (a)Al-6.5Si [24] (b)Al-12Si [25] (c)Al-18Si [24]

2.1.3 POROSITY OF SPRAY DEPOSITED ALLOYS

The presence of some porosity is inevitable in spray formed materials [14]. Following are the types of porosity present in spray deposited material:

2.1.3.1 Interstitial porosity: - Upon impingement, solidified individual droplets overlap each other, forming interstices. If the fraction of liquid in the incident spray is too low, these interstices will not be completely filled by the liquid, which will lead to porosity formation. Indeed, it was recently suggested that the low level of porosity achieved with a novel spray forming technique can be most likely attributed to the fact that an optimal fraction of solid is maintained under a controlled pressure environment. The formation of interstitial porosity is dependent on both the amount of liquid present in the deposit and the thermal condition present on the substrate during deposition. The interstitial porosity would depend on the packing characteristics of the droplets.

2.1.3.2 Gas entrapment: - When the atomised droplets impinge on the upper layer of the deposit formed by the preceding droplet, and containing relatively higher amounts of liquid, the surface is continuously disturbed by the high velocity gas jet, and the gas may be mechanically entrapped, resulting in entrapped gas porosity.

2.1.3.3 Porosity associated with solidification (solidification porosity): - Solidification porosity is significant when too much liquid is present in the spray upon impingement, interstitial porosity and solidification porosity may be treated as two mutually exclusive occurrences.

2.1.3.4 Intersplat boundary: - Atomised droplets formed splats, when they impinge on the substrate. This illustrates that a fraction of the atomised droplets arriving at the deposition surface were in the partly liquid partly solid state. In most cases, the major axis of the splat was parallel to the substrate surface. However, in some cases the orientation of the splat vis-a`-vis substrate surface was such that the major axis of the splat was not horizontal. It was observed that in some areas the two consecutive splats joined together with very little porosity at the interface, while in some other there were significant amounts of porosity at the interface. There were also areas, in which a number of discrete pores were present on the splat boundary. This leads to the formation of intersplat boundary porosity.

2.1.3.5 Porosity due to hydrogen evolution: - The atomising gas may get dissolved in molten metal. Generally, the solubility of gas decreases as the metal solidifies. The dissolved gas would evolve during solidification. If the solidification velocity is more than the diffusive

velocity of the evolved gas, gas pores would form. Such type of porosity would be related to the amount of liquid fraction present. In the present study, aluminium was spray deposited with nitrogen. The solubility of oxygen and nitrogen in aluminium is extremely small. The only gas which is soluble in aluminium in significant amounts is hydrogen.

The formation of porosity during spray forming is influenced by many factors including processing parameters, thermodynamic properties of the materials, thermodynamic properties of the atomization gases, as well as considerations pertaining to apparatus design. There are effects of various process parameters on porosity of spray deposited Al-Si-Gr composite such as atomising pressure, deposition distance, melt superheat and melt delivery tube diameter on porosity of the spray deposited Al-Si-Gr composite.

Underhill et al. [49] found that the porosity increases with the increase in deposition rate, the decrease in atomising gas pressure, and the decrease in deposition distance. [13]

2.2 FRICTION STIR PROCESSING

Friction stir processing is used to refine the grain. The tool consists of a small sized cylindrical pin and concentric large diameter shoulder generally the shoulder diameter should be greater than or equal to three times the sheet thickness. When the tool is plunged into the sample, the rotating pin contacts with the upper surface and generates frictional heat between the sheet surface and the shoulder. Frictional heating of the material, makes it soft in the small column of pin movement (stir zone). The tool shoulder diameter and the length of the pin controls the depth of penetration. The higher the ratio of rpm and traverse speed, greater is the heat input [35].

Fig. 2.3 Photograph of FSP machine

2.2.1 HISTORY OF FRICTION STIR PROCESSING

Friction stir welding (FSW) was invented in 1991 at The Welding Institute of UK. It is a solid state welding technique and initially FSW was used to join only Al alloys [36,37]. Recently Mishra et al. [38,39] has observed that surface modification of many metals (i.e. Al alloys, Mg alloys, steel) can be done by using the same basic principle of FSW and thus a new surface modification technique has been developed and named as friction stir processing (FSP). Friction stir processing (FSP) is related to the friction stir welding (FSW) technique developed at TWI [36]. FSP has shown significant microstructural refinement and improved mechanical properties for both wrought aluminium alloys and cast microstructures.

2.2.2 THE MICROSTRUCTURAL AND MACROSTRUCTURAL EVOLUTION DURING FSP

The softened material flow from the advancing side to the retreating side by the rotary and traverse movement of the tool. Al-Si alloys are highly recommended to be used in aerospace application due to their high strength, good corrosion resistance and excellent cast ability but some mechanical properties of the cast alloy (for example -ductility, fatigue life and toughness) are limited due to porosity, coarse Si particles and large Al dendrites. As the eutectic Si and the primary Si have low toughness value, so they act as a stress concentration source. And when a crack is initiated in the Si region, then crack starts to propagate through the continuous wall of Si, which causes low ductility value of the cast metal.

Various heat treatment techniques have been developed to modify the microstructure of the cast Al-Si alloy but among all of them FSP have shown great results. The stirring action causes break down of coarse Si particles and Al dendrites. Thus an improvement can be seen in ductility after FSP.

Karthikeyan et al. [40] have performed single pass FSP on cast A319. During the processing, three different tool traverse speeds viz. 22.2 mm/min, 40.2 mm/min and 75 mm/min and five different tool rotational speeds viz. 800 rpm, 1000 rpm, 1200 rpm, 1400 rpm and 1600 rpm was used. It has been observed that both tool rotational and traverse speed affect the microstructure and mechanical properties of castA319 alloy. The author proposed that if tool rotational and traverse speed is very high or very low then defective stir zone (SZ) forms. To get defect free SZ a perfect combination of traverse speed and tool rotational speed have to be chosen. The author observed that best properties were obtained by using tool rotational speed of 1200 rpm. After FSP, cast A319 alloy have shown good improvement in ductility, yield strength and hardness. Ma et al. [41] performed FSP on cast A356 alloy to understand the effect of tool rotational and traverse speed on the microstructure and mechanical properties of the alloy. They revealed that coarse Si particle and dendrites of Al breaks due to the stirring action of the tool. FSP causes formation of fine grains of 3-4 μm. They found that process parameters do not influence the size of the grains in the stir zone but have a significant effect on the microstructure of the SZ. Basin like stir zone stir zone creates due to low rotational speed (300-500 rpm) but high rotational speed creates an elliptical processed zone. Low density of Si particles which makes an optically visible banded structure on the SZ was found due to low rotational speed/traverse speed ratio. High tool rotational speed causes homogeneous distribution of Si particles. Gandra et al. [42] performed multipass FSP on AA

5083-H111 alloy to find out effect of overlapping direction on the microstructure and mechanical properties of the alloy. During the process, the tool rotation and traverse speed was maintained at 1000 rpm and 25 mm/sec respectively. The test reveals that overlapping by advancing side (AS) produce more irregular surface finishing. Hardness value in both cases remains almost constant. Best bending test result was obtained in the samples which were overlapped by the advancing side (AS). Rao et al. [43] performed FSP on cast hypereutectic Al-30Si alloy to understand the effect of two pass overlap FSP on microstructural refinement of the subjected alloy. The second pass was done with 100% overlap over the first pass. Throughout the process the tool rotational and traverse speed was 1000 rpm and 16 mm/min respectively. The experiment reveals that the stirring action during the process causes significant break up of undesirable coarse primary and eutectic Si particles. The double pass causes more homogenous distribution of Si particles. Hardness of the material at double pass processed zone was slightly higher than the single pass processed zone. Tsai et al. [44] have conducted single pass FSP on solution treated AC8A alloy. The tool rotation and traverse speed was maintained at 1400 rpm and 45 mm/min respectively during the process. The mechanical properties of the friction stir processed sample (especially the elongation value) were significantly improved. The author observed that the processing parameters significantly affect the mechanical properties of the processed samples and high tool rotation and traverse speed causes more strength in the specimen. Santella et al. [45] how the FSP affect the mechanical properties of as- cast A356 and A319 alloy. During the process, the tool rotational and traverse speed was maintained at 1000 rpm and 1.7 mm/sec. respectively. Some bars were processed 5-6 passes overlapped on intervals of about 4 mm. It has been observed that the dendritic structure and coarse Si particles were broken after FSP. Moreover, it has been concluded that visible porosity was eliminated which results in significant improvement in UTS value, ductility and fatigue lives of both alloy. Micro hardness distribution in the stir zone was more uniform. Mahmud et al. [46] investigated that how tool rotational speed and transverse effects on the microstructure, mechanical properties and tribological characteristic of cast A390 alloy. The result reveals that after FSP, some casting defect (i.e. porosity) was eliminated. The author concluded that FSP causes refinement of grains and coarse Si particles. FSP can reduce the mean size and aspect ratio of the Si particles. The author also concludes that the higher tool rotational speed and/or lower traverse speed causes the increment of the mean size of the Si particles. But if the number of passes increases than the mean size of the Si particle will decrease. The minimum size and aspect ratio of the Si particles was obtained by processing at tool rotational speed of 1200 rpm and traverse speed of 20mm/min with three passes. The as-

cast A390 sample shows scattered hardness value. But after FSP the hardness value of the sample was less scattered and higher than the parent material. The above mentioned process parameters causes maximum increment in hardness value. The author also concluded that the hardness value of the processed zone increases with increasing the traverse speed and number of passes. Karthikeyan et al. [47] have done FSP on as-cast aluminium 2285 alloy to study the effect of process parameters on the mechanical properties of the cast alloy. The author has concluded that FSP causes improvement in mechanical properties by removing the casting defects and by modifying the microstructure of the cast alloy. Three different traverse speeds viz. 10 mm/min, 12 mm/min and 15 mm/min with two different tool rotational speeds viz. 1400 rpm and 1800 rpm were used during the process. Around thirty percent improvement was observed in yield strength and ultimate tensile strength (UTS) after processing. Ductility of the parent material was increased around four fold after FSP. The tool rotational and traverse speed significantly affect the final microstructure of the parent material and thus affect the mechanical properties. Samples processed with tool rotational speed of 1800 rpm and traverse speed of 12 mm/min have shown the best mechanical properties. Some attempt has been done to find out the effect of processing parameters on the abnormal growth of grains during friction stir processing. Kapoor et al. [48] has investigated the effect of FSP on the tensile and fatigue properties of cast A206 alloy. The author has observed that FSP can eliminate porosity. The stirring action during the process causes breakdown of coarse Si particles and refinement of grains. After FSP, the UTS and ductility value of the parent material has been improved but no significant change has been observed in yield strength. The investigator has concluded that heat treatment did not shown much effect on UTS value.

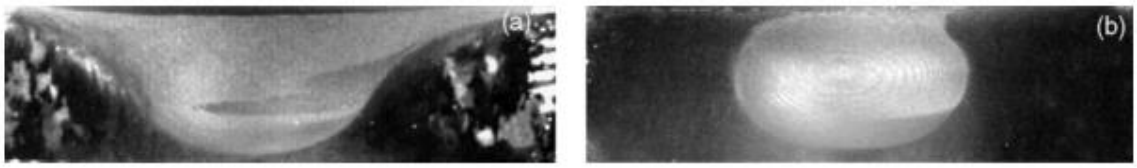

Fig. 2.4 Macrostructure of nugget shape in FSP A356:(a) basin like stir zone (b)onion like stir zone [35]

Maximum heat is generated in the stir zone. Due to high heat and intense plastic deformation, the grains of stir zone are fully recrystallized due to which this zone is also known as dynamically recrystallized zone(DRZ) [34]. The dislocation density of the interior of the recrystallized grains is low [32,33]. Although some authors reported that small recrystallized

grains of the stir zone have high density of sub grain and dislocation [31]. Stir zone have an onion like or basin like structure as shown in Fig. 2.4

2.2.3 ELIMINATION OF POROSITY BY FSP

Mishra et al. [35] investigated the effect of FSP on microstructure of A356. FSP eliminated the porosity in the as-cast A356. The material within the processed zone of the FSP A356 experienced intense stirring and mixing, thereby resulting in breakup of the coarse acicular Si particles and dendrite structure and homogeneous distribution of the Si particles throughout the aluminium matrix. During FSP, tool transports materials from the front to the back of the tool in a complex way, resulting in intense deformation and mixing of material. It is expected that such a process can refine effectively the microstructure of Al–Si–Mg castings.

Recently, Ma et al. [41] investigated the effect of FSP on microstructure and properties of A356. FSP resulted in a significant breakup of coarse acicular Si particles and primary aluminium dendrites, created a homogeneous distribution of Si particles in the aluminium matrix, and nearly eliminated all casting porosity. FSP completely eliminated porosity in cast A356 alloy.

T.S. Mahmoud [46] investigated the effect of FSP on properties of A390 Al alloy. Microstructural analysis clearly indicated intrinsic heterogeneity in terms of both porosity and primary Si particles associated with the as-cast A390 Al alloy. Defects like porosity, cracks, and blow holes lead to a reduction in the strength and hardness of cast aluminium–silicon alloys. Increasing the tool rotational speed and/or reducing the tool traverse speed increase(s) the frictional heat during FSP which resulted in an increase of the size of the recrystallized a-Al grains.

2.2.4 STRENGTHENING MECHANISMS IN FRICTION STIR PROCESSED COMPOSITES

FSP has been utilised to refine the microstructure of different metal matrix composite and enhance mechanical properties. As a result of the plastic deformation at elevated temperatures, in-situ intermetallic are formed during FSP. The orowan strengthening from these nano sized intermetallic phase, grain boundary strengthening and the load shearing effect of the reinforcements, contribute to the high composite strength. Orowan strengthening is basically the intragranular interaction between the Nano sized intermetallic particles with the dislocations. This has a hindering action on the dislocation movement thereby enhancing its strength. The equation for Orowan strengthening [3,4] is given by following equation.

$$\tau_{OR} = \frac{0.81Gb}{2\pi(1-\nu)^{1/2}\lambda} \ln\left(2\sqrt{2/3}r / r_0\right) \tag{2.1}$$

Where **G** is the matrix shear modulus, **b** is the Burgers vector, ν is the Poisson's ratio and $\mathbf{r_0}$(=4b) is the dislocation core radius and **λ** is the inter-particle spacing. Higher the reinforcement content, more is the Orowan strengthening effect.

The grain boundary strengthening is based on the Hall-Petch's equation. [5] The significance is that with increase in the ratio of rotating speed to traverse speed. Generally, the flow stress of the matrix decreases. Hence, the grains do not fragment readily and grow in size with increase in the ratio. In some cases, however, with higher rotating speed, the strain rate also increases and the grains may refine as well depending on the dominance of strain rate over temperature attained. The strength of the composite is thus greatly influenced by this ratio.

Load sharing effect is based on the Halpin-Tsai equation [30]. The Young's modulus of elasticity for a composite increase with the increase in the reinforcement content.

$$E_2 = \frac{E_m(1+\xi\eta f)}{1-\eta f} \tag{2.2}$$

Where, E_2, E_m and E_f are the young's moduli of the composite, matrix and reinforcement respectively, ξ is an adjustable parameter and f is the volume fraction of the particles. In the equation (2) value of η is,

$$\eta = \frac{(\frac{E_f}{E_m} - 1)}{(\frac{E_f}{E_m} + \xi)} \tag{2.3}$$

CHAPTER 3
PLAN OF WORK

3.1 OBJECTIVES OF PRESENT RESEARCH WORK

This research work is done with the following objectives:

1. Producing a homogeneous, fine-grained Al-Si-Gr composite with good mechanical properties for the cylindrical linings application.
2. Reducing the porosity of the spray deposited material through FSP.
3. Grain Refinement of the spray formed composite with the help of FSP.
4. To study the microstructural variations in the formed composite, before and after FSP.
5. To study the mechanical properties, present in the spray formed and FSPed composites.

The aim was to produce homogeneous, fine-grained Al-Si-Gr composite and then, reduce the porosity of the highly porous Al-Si-Gr composite formed by the spray forming through FSP and hence refining its microstructure and enhancing its mechanical properties like wear resistance, tensile strength and hardness.

A lot of methods have been used in the past to reduce porosity of the spray formed material. But there is no research work available to show effect of friction stir processing on spray formed material. The plan of work starts with setting up spray forming chamber, friction stir processing machine and optimizing parameters of spray forming process and FS-process.

3.2 SETUP

3.2.1 SPRAY FORMING

Design and fabrication of spray forming setup is developed indigenously. Free fall type atomiser was mounted on the inner side of the top surface plate of the spray deposition chamber in such a way that the central vertical axes of the atomiser and the melt delivery tube coincided with each other. It mainly consisted of induction furnace, atomizer, melt delivery tube and substrate.

3.2.2 FRICTION STIR PROCESSING

Fabrication and design of FSP setup is developed indigenously. It mainly consisted of round table which rotates in both CW and CCW direction. The table can be rotated easily by rotating hand wheel using worm, wheel mechanism. The setup is made from gears cut from cast iron and bearings are made of MS (mild steel) with case hardening.

3.3 PARAMETERS OPTIMIZATION

3.3.1 SPRAY FORMING

There are various parameters present the spray forming process which control the properties of the material formed. These all parameters must be according to the application of the material for which we are producing it. These parameters are weight of the alloy for each run, melt delivery tube diameter, angle of the substrate, substrate rotational speed, air gas pressure, melt temperature and distance from the substrate to atomizer. There are various models available in the literature which are used to find the optimized parameters for our research work.

3.3.2 FRICTION STIR PROCESSING

Basically, there are two types of parameter present in this process. These are process parameter and tool parameters. Process parameter like tilt angle, traverse speed and rotational speed are optimized using the previous literature work. The conditions are selected, so as to provide the best possible properties in the FSPed material. The tool selected for FSP is from the point of view of both strength and necessity of the amount of material required for our research work.

CHAPTER 4
EXPERIMENTAL PROCEDURE

4.1 MATERIALS

The base alloy used in the present work consisted of Al-Si alloy having 30% Si. We've used graphite powder of 1-5 μm size. The alloy used was superheated to 150ºC above its melting point temperature in graphite crucible using an induction furnace. We've produced Al-6Si-5Gr, Al-12Si-5Gr and Al-18Si-5Gr by mixing base alloy with pure Al in exact ratios. Graphite powder was mixed in alloy at the time of run. In each run 950 gm of Al-Si alloy was taken in crucible and 50 gram of graphite was taken in funnel. Following table shows the amount of base alloy, pure Al and graphite powder used to make this composites.

Table 4.1 Mixing amounts of Base alloy, Pure Al and Graphite

	Al-30Si	Pure Al (Al>99%)	Graphite
Al-6Si-5Gr	200 grams	750 grams	50 grams
Al-12Si-5Gr	400 grams	550 grams	50 grams
Al-18Si-5Gr	600 grams	350 grams	50 grams

4.2 SPRAY FORMING

The Al-Si alloys of different composition were melted in graphite crucible one by one inside a high temperature furnace. At centre of the bottom of the crucible an exchangeable graphite melt delivery tube was fitted to produce melt flow stream. Continuous Stirring was performed to properly mix the liquid miscible alloys. A stopper rod was used to either open or close the entrance of the delivery tube. Bottom end of the delivery tube was fitted into the atomizer, which was placed at 350 mm above the substrate.

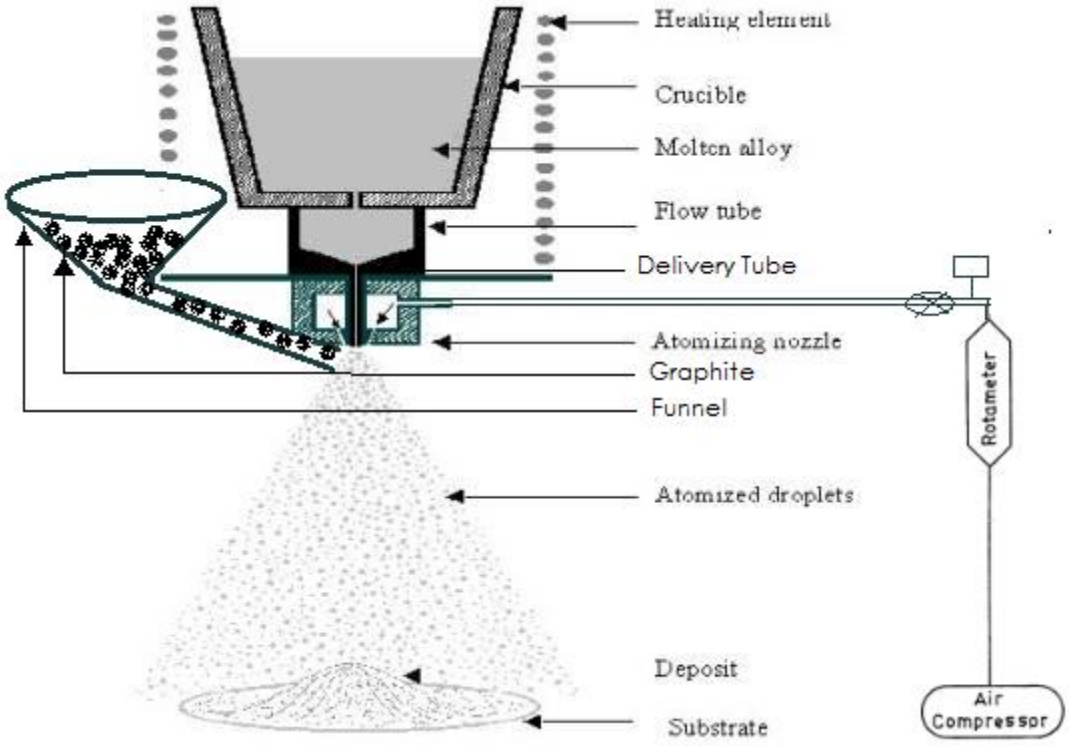

Fig. 4.1 Spray Forming

Three successful spray forming experiment were conducted. At the start of each experiment, stopper rod was raised up after starting the high pressure gas flow in atomizer to start the atomization of the Al-Si melt. Vertically falling liquid metal stream is atomized into spray of small size droplets. The gas at high pressure interacts with liquid metal as it comes out of delivery tube and splits it into fine droplets. μm size graphite particles were mixed into these droplets by allowing the graphite particles to fall through a funnel into the spray as shown in schematic diagram. These fine droplets solidify and get deposited over horizontal copper substrate of diameter 200mm which was rotating at 240 rpm.

Delivery tubes used in our experiment have Internal diameter=5mm and Length of tube=70mm. The pictures of atomizer and delivery tube used in our study is shown in fig. 4.2 and fig. 4.3 respectively.

Fig. 4.2 Picture of closed type gas atomizer used in spray forming

Fig. 4.3 Picture of delivery tube

Table 4.2 Parameters used in spray forming process

Parameters of the process	Value of the parameters		
	Al-6Si-5Gr	Al-12Si-5Gr	Al-18Si-5Gr
Weight of the alloy for each run	1000 grams	1000 grams	1000 grams
Melt Delivery Tube Diameter	5 mm	5 mm	5 mm
Substrate Thickness	8 mm	8 mm	8 mm
Angle of the Substrate	0º	0º	0º
Substrate Diameter	200 mm	200 mm	200 mm
Substrate rotational speed	240 rpm	240 rpm	240 rpm
Air gas pressure	0.7 MPa	0.7 MPa	0.7 MPa
Melt Temperature	790ºC	725ºC	822ºC
Distance from the substrate to atomizer	350 mm	350 mm	350 mm

The shape of spray deposited material collected over horizontal copper substrate is as shown in fig. 4.4.

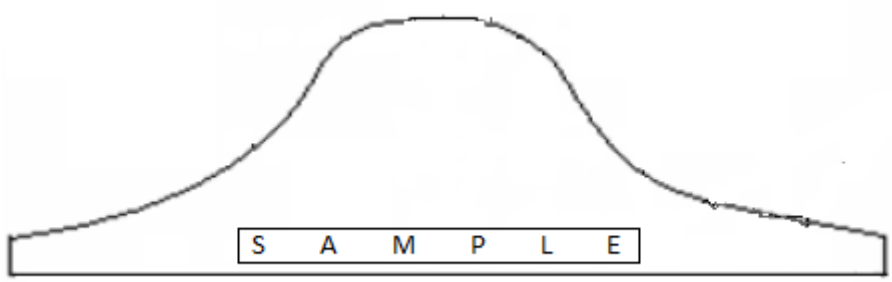

Fig. 4.4 Spray deposit's shape collected over substrate

4.3 FRICTION STIR PROCESSING

A vertical milling machine was used to perform FSP. A 3 Horse Power (HP) motor was mounted on the top of the milling machine which allows having eight variable spindle speeds. There was a gear in the machine by which we can easily adjust speed. There was a semi-automatic adjustable table by which traverse speed and plunge depth can be maintained at optimum level. The milling machine was modified with work piece fixture and tool holder to perform FSP. The setup used for FSP is shown in fig. 4.5.

The Spray formed composite was cut into rectangular plates of thickness 1cm from the region marked as 'SAMPLE' in rectangle in Fig. 4.4. The FSP was performed on the centre region of the plates. Tool used for FSP was decided from the point of view of our required results. Tool used were of high strength. FSP carried out at constant parameters for all samples so that a clear comparison would be made. A die steel tool was used for processing with shoulder diameter 22 mm, a cylindrical pin with 6 mm diameter and height of 2 mm length. A tilt of 2^{o} was provided for easy movement of tool over plate and having good material flow.

The 1025 rpm rotational speed and 50 mm/min traverse speed indicate high heat generating conditions. The traverse speed (50 mm/min) and rotational speed (1025 rpm) were same for processing composite compositions. The nugget layer was extracted from the friction stir processed zone. Removing of 2 mm thickness from the upper side or processed side was

done mechanically, then this 2 mm thick nugget layer is used for different characterization and mechanical tests.

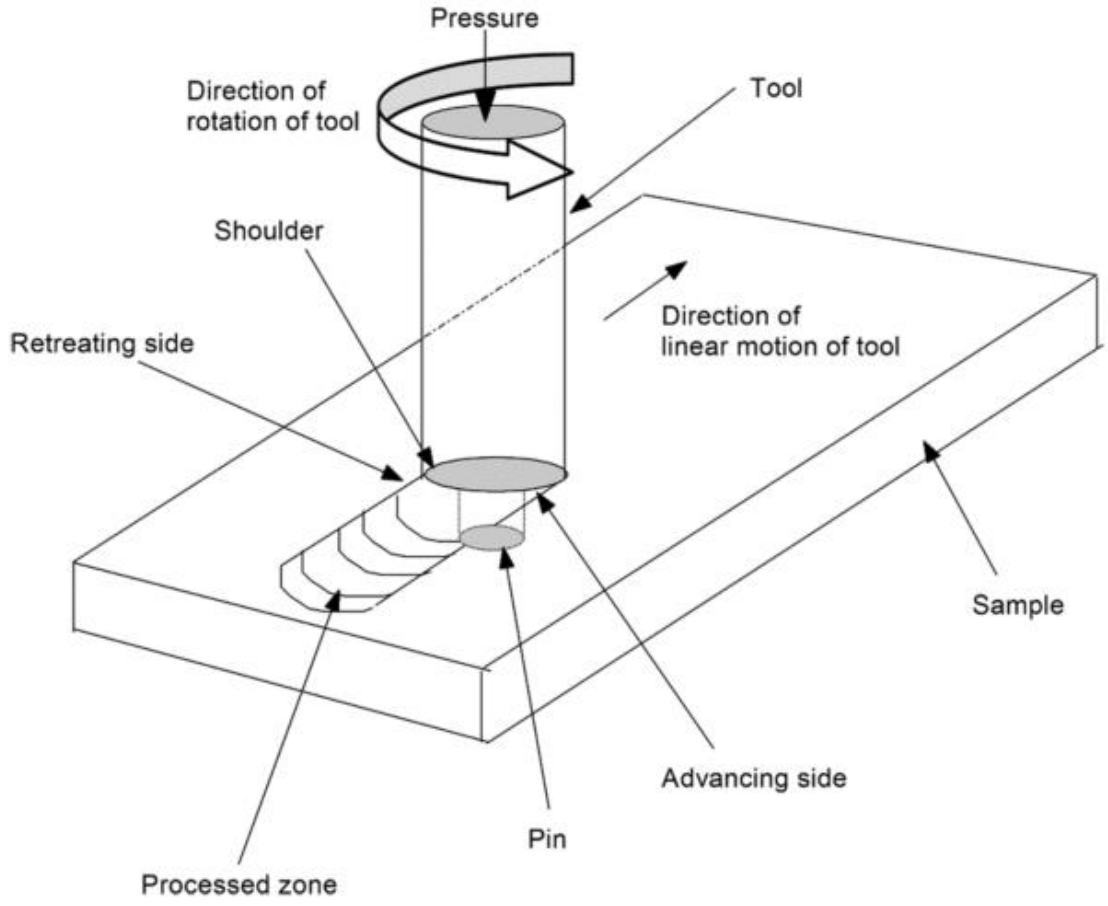

Fig. 4.5 Friction Stir Processing

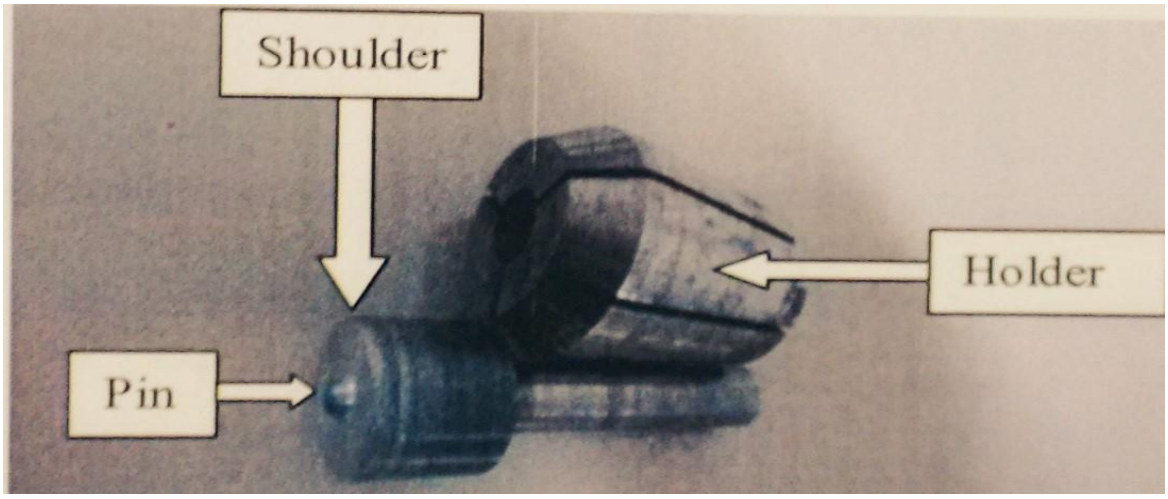

Fig. 4.6 Holder and tool used during FSP

4.4 POROSITY

For the calculations of porosity, measured density is calculated through Archimedes principle set-up and theoretical density through ASTM B 328 96. The calculated theoretical density from the ASTM standard is shown in Table 4.3.

Table 4.3: Theoretical Density

Al-18Si-5Gr	2.61152
Al-12Si-5Gr	2.63378
Al-6Si-5Gr	2.65604

Porosity is measured using the formula given below [13].

$$\boldsymbol{Porosity = 1 - \frac{Measured\ density}{Theoretical\ Density}} \tag{4.1}$$

The values reported in results are mean values of three measurements. In addition to this the surface porosity is measured using the computer software 'Dewinter material plus' from the optical microscope images.

4.5 MATERIALS CHARACTERIZATION

Samples were polished with grit SiC papers of grit sizes 320, 800, 1200, 1500 and 2000 then followed by wheel cloth polishing using an emulsion of Magnesium Oxide (MgO) powder particles suspended in water. Keller's reagent is used to etch aluminum alloys to reveal their grain boundaries and orientations. It is also sometimes called as Dix-Keller reagent.

4.5.1 OPTICAL MICROSCOPY

A Leica DMI 500M microscope was used to find the images for studying microstructure. This is a simple microscope which uses visible light spectrum and a system of magnifying lenses to produce images.

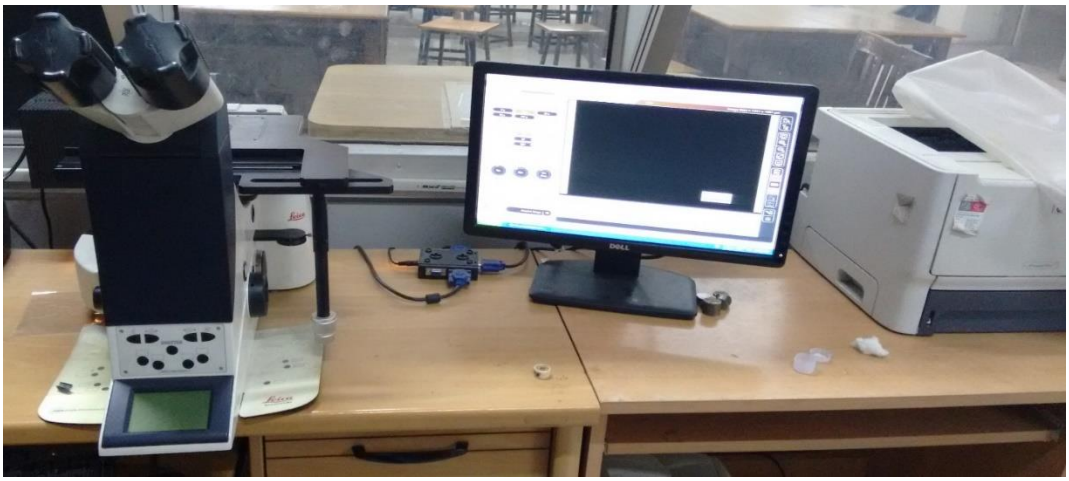

Fig. 4.7 Leica DMI 500M optical microscope

4.5.2 SEM MICROSCOPY

Microstructural and morphological characteristics were studied with the help of scanning electron microscope.

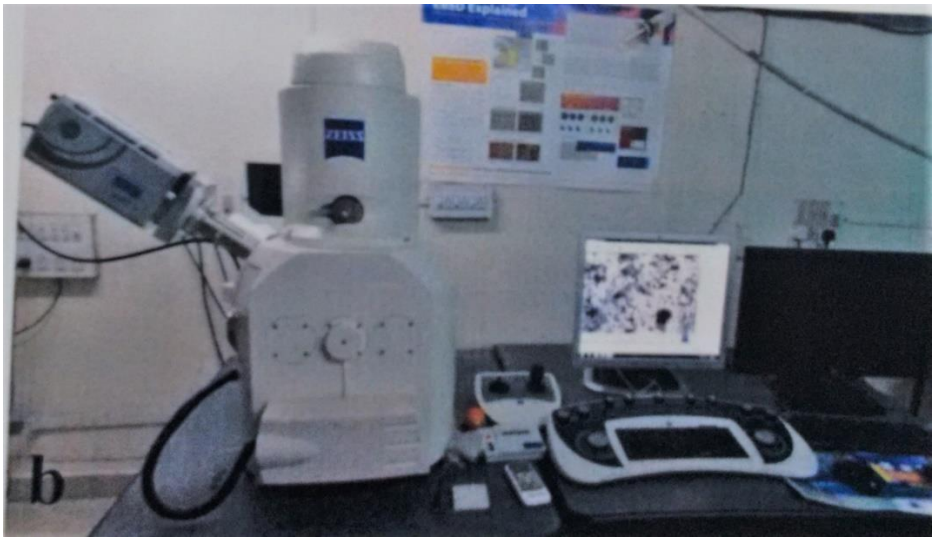

Fig. 4.8 SEM (scanning electron microscope)

4.5.3 EDAX ANALYSIS

Graphite distribution was checked through EDAX analysis technique in all three spray deposited composites and further analysis was done after FSP.

4.5.4 XRD ANALYSIS

XRD analysis of spray deposit for different composition of silicon viz. 6, 12 and 18% in Al-Si-5Gr composite was carried out by Rigaku X-Ray diffractometer, using copper target and nickel filter. Diffraction angle (2 θ) was varied from 20º to 120º in step of 0.05 deg. The Goniometer speed was 2º/min.

Fig. 4.9 X-ray diffractometer

4.6 MECHANICAL TESTING

Different mechanical properties of the spray formed composite were measured and the changes produced in mechanical properties after FSP were also measured. Hardness and tensile strength were measured.

4.6.1 HARDNESS

The hardness was measured using a computerized Vickers hardness testing machine. The sample were well polished before measuring hardness using standard metallographic technique. A load of 1 kgf was applied with a dwell time of 15 seconds to measure hardness in machine. The hardness values reported in results are mean values of the three measurements. The effect of FSP on Vickers hardness of the spray deposited Al-Si-Gr composites were measured for all samples.

Fig. 4.10 Vickers's hardness testing machine

4.6.2 TENSILE TESTING

Tensile test was done on universal testing machine (Tinius Olsen, Model:H25KS) with 0.5 mm/minute rate of pulling specimen. The tensile specimen used for testing is shown in fig.4.11.

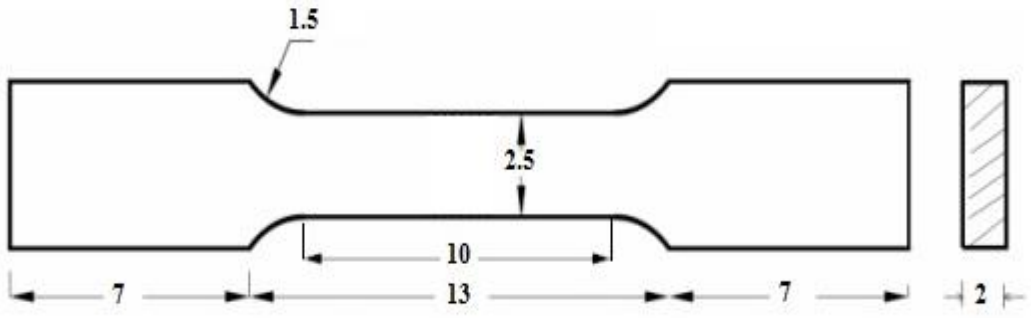

Fig. 4.11 Schematic illustration of Tensile test specimen

Tensile test was done at all compositions, before and after FSP. The values of the yield point and ultimate tensile strength recorded are the mean values of three measurements.

Fig. 4.12 Universal testing machine (Tinius Olsen, Model:H25KS)

CHAPTER 5
RESULTS AND DISCUSSION

5.1 POROSITY

There is effect of various process parameters such as atomising pressure, deposition distance, melt superheat and melt delivery tube diameter on porosity of the spray deposited Al-Si-Gr composite. There are several types of porosity present in the composite, namely interstitial, mechanically entrapped gas, intersplat boundary, solidification shrinkage and porosity due to hydrogen evolution [14]. Porosity is detrimental because it can significantly reduce strength, toughness, hardness and other properties. High gas velocity can lead to the more gas entrapment of the gas in the deposit.

Table 5.1 Determined porosity values

Material	Theoretical Density(kg/m^3)	Actual Density(kg/m^3)	Porosity in Percent
Al-18Si-5Gr (Spray formed)	2611.52	2171.51	16.85
Al-12Si-5Gr (Spray formed)	2633.78	2205.72	16.25
Al-6Si-5Gr (Spray formed)	2656.04	2238.16	15.73
Al-18Si-5Gr (Friction stir processed)	2611.52	2444.28	6.40
Al-12Si-5Gr (Friction stir processed)	2633.78	2474.01	6.06
Al-6Si-5Gr (Friction stir processed)	2656.04	2501.84	5.80

We see that, there is about 70% decrease in porosity after FSP, this is due to the hot working nature and stirring action which causes the reduction in porosity of the spray formed sample. Forward motion of tool results in closure of pores present in spray formed composite. The FSP's rotating tool served following two important purposes. Heating of the composite by

developing frictional heat between tool and composite and stirring of the composite. As a result, there is removal of porosity.

5.2 MICROSTRUCTURAL FEATURES

Fig. 5.1 shows the optical micrographs obtained from light microscope at 20X magnification. The optical micrographs show white region as aluminium and grey contrast region as eutectic silicon. Primary silicon can be seen in hyper-eutectic alloy as small spherical particles suspended homogeneously in Al-matrix in high contrast grey colour compared to eutectic silicon. Graphite particles are too small to be seen in this resolution.

Silicon is soluble in Aluminium in liquid state. No macro segregation of silicon is seen in composite macrostructure. Cooling of liquid takes place during their flight in gas stream. Some droplets fully solidify, some partially and other remain in liquid state before deposition on the copper substrate to form the spray deposited Al-Si-Gr composite. In this way, Spray forming produces fine scale microstructure, which is refined and equiaxed. Slow cooling in casting results in coarse and segregated microstructure. Spray generates μm size droplets. Rapid solidification effects inherent in spray deposition by providing a significant chemical and microstructural homogeneity along with refinement of grains and second phase particle size. The eutectic phase exhibited divorced morphology as a result of high interfacial energy between the two component phases. The average grain size found in the spray formed samples is 25-45 μm. Whereas grain size of primary silicon in hyper-eutectic alloy was found to be of 5-15 μm.

Equiaxed grains of primary aluminium were observed and silicon was present within these grains and along the grain boundary. With the increase in silicon content in the composite, we see that more primary silicon is present in the grain boundary.

Fig. 5.2-5.4 shows SEM micrographs at 5000X magnification for different compositions of spray formed material and changes produced in it by FSP. We see there is no presence of primary silicon in Al-6Si-5Gr and Al-12Si-5Gr because of the less concentration of silicon than eutectic point. In the case hypereutectic Al-18Si-5Gr, point EDAX analysis clearly revealed the presence of primary silicon and eutectic silicon phases in the composite. In these images we majorly see grey portion, which is aluminium matrix. The white region is silicon phase. The black region shows porosity and graphite particles. The size of primary silicon was found to be larger than eutectic silicon in hypereutectic case and the size of eutectic

silicon in hypereutectic case was found to be larger than eutectic and hypoeutectic Al-Si alloy compositions.

Semi-solid or semi-liquid metal mass is continuously depositing and solidifying on the copper substrate deposition surface. This continuously depositing composite mass will release heat quickly to the surroundings having high speed gas velocity, and already/previously deposited mass. The high speed gas velocity leads to the high rate of heat transfer by convection and previously deposited mass leads to high rate of heat transfer by conduction from the depositing mass. Therefore, the formation of nuclei in the composite and high rate of heat transfer from the melt leads to very fast solidification rate of spray deposit and thereby formation of equiaxed structure. The silicon in the structure of composite is in particulate form opposite to the conventional cast structure. It also indicates rapid solidification of the deposit. [19] [20]

The FSP's rotating tool served following two important purposes. The heating of the composite by developing frictional heat between the tool and composite and stirring of the composite. As a result, there is removal of porosity and proper homogenisation. Microstructure of nugget zone of FSPed samples reveal further grain refinement of composite. The nappy fashion shows the complex nature of the material throughout the processing. The average grain size in the stir zone is 5-20 μm and the size of primary silicon particles in the hyper-eutectic region is 2-4 μm.

We can see that grain boundaries are not clear after FSP. This happens because of very small grain size of the material.

Dendritic microstructures which are present in small amount in spray deposited material are removed after FSP. This creates uniform distribution of Silicon throughout the matrix. FSP has reduced the grain size of spray formed sample from 25-45 μm to 5-20 μm. It can be seen that graphite distribution is uniform throughout the aluminium matrix. Size of primary silicon in hypereutectic alloy is reduced from 5-15 μm to 2-4 μm.

No porosity greater than 1 μm was observed in FSPed specimen.

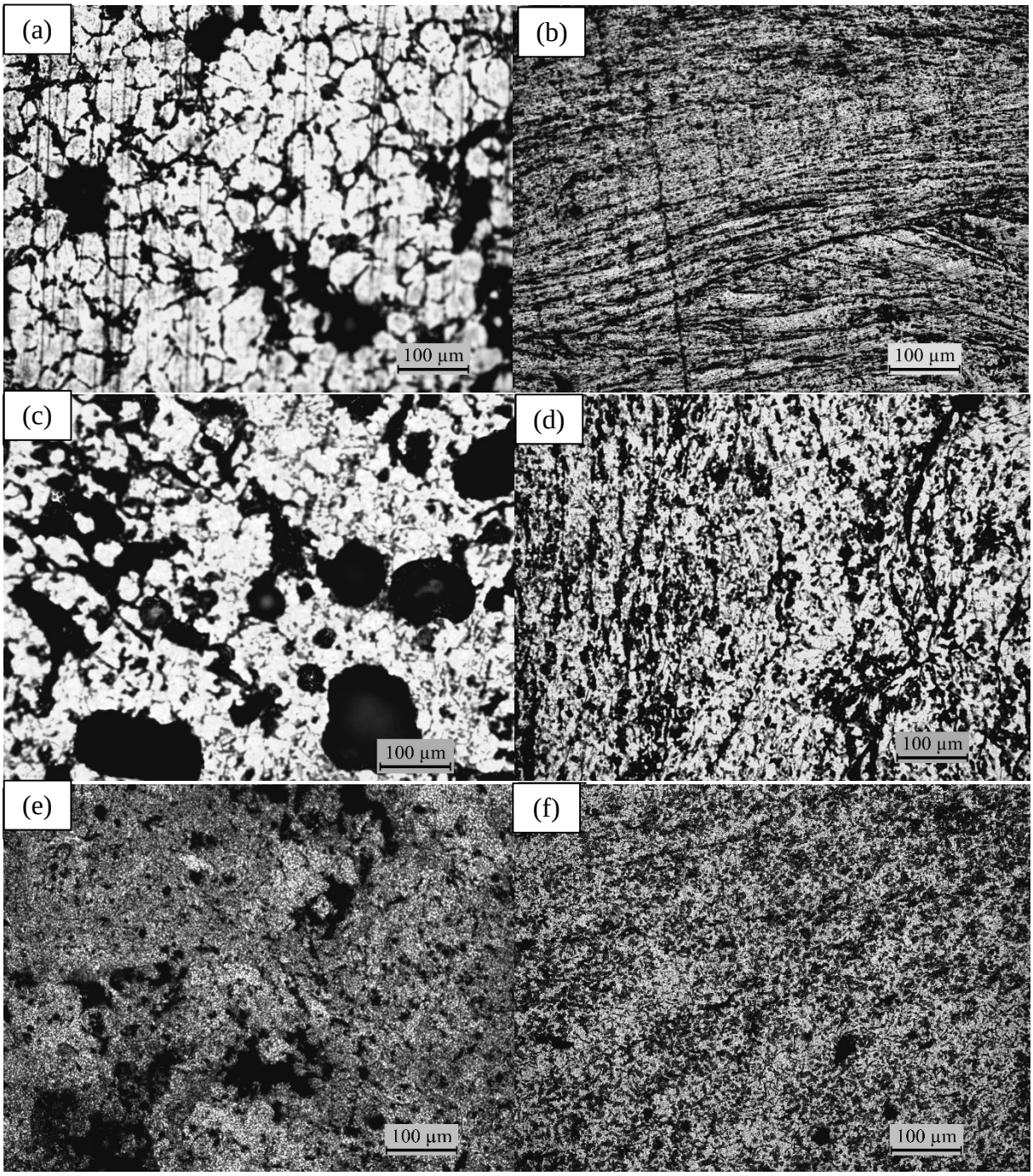

Fig. 5.1 Optical Micrographs of (a) Spray Formed Al-6Si-5Gr (b) Friction Stir Processed Al-6Si-5Gr (c) Spray Formed Al-12Si-5Gr (d) Friction Stir Processed Al-12Si-5Gr (e) Spray Formed Al-18Si-5Gr (f) Friction Stir Processed Al-18Si-5Gr

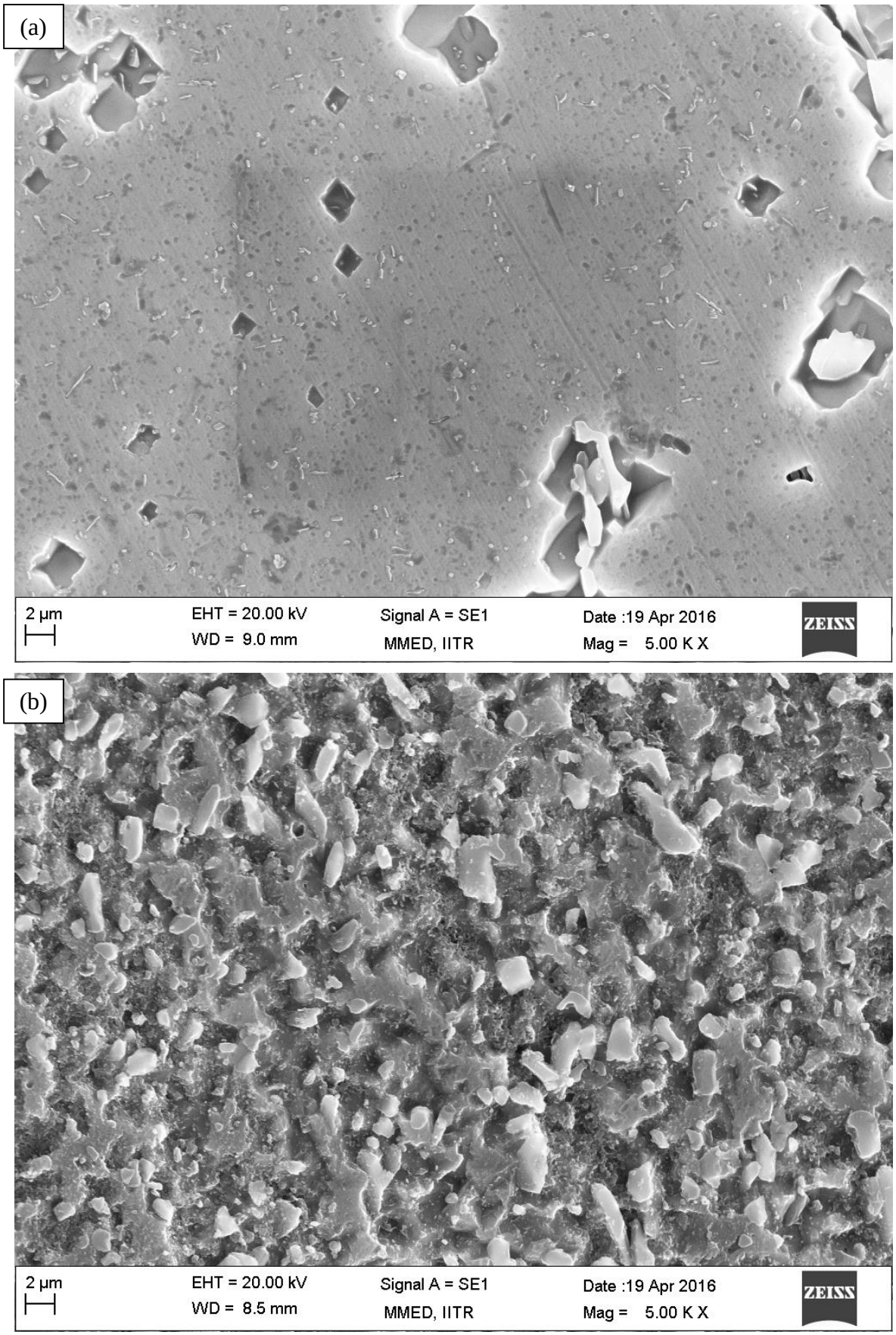

Fig. 5.2 SEM micrograph of Al-6Si-5Gr (a) Spray Formed (b) FSPed

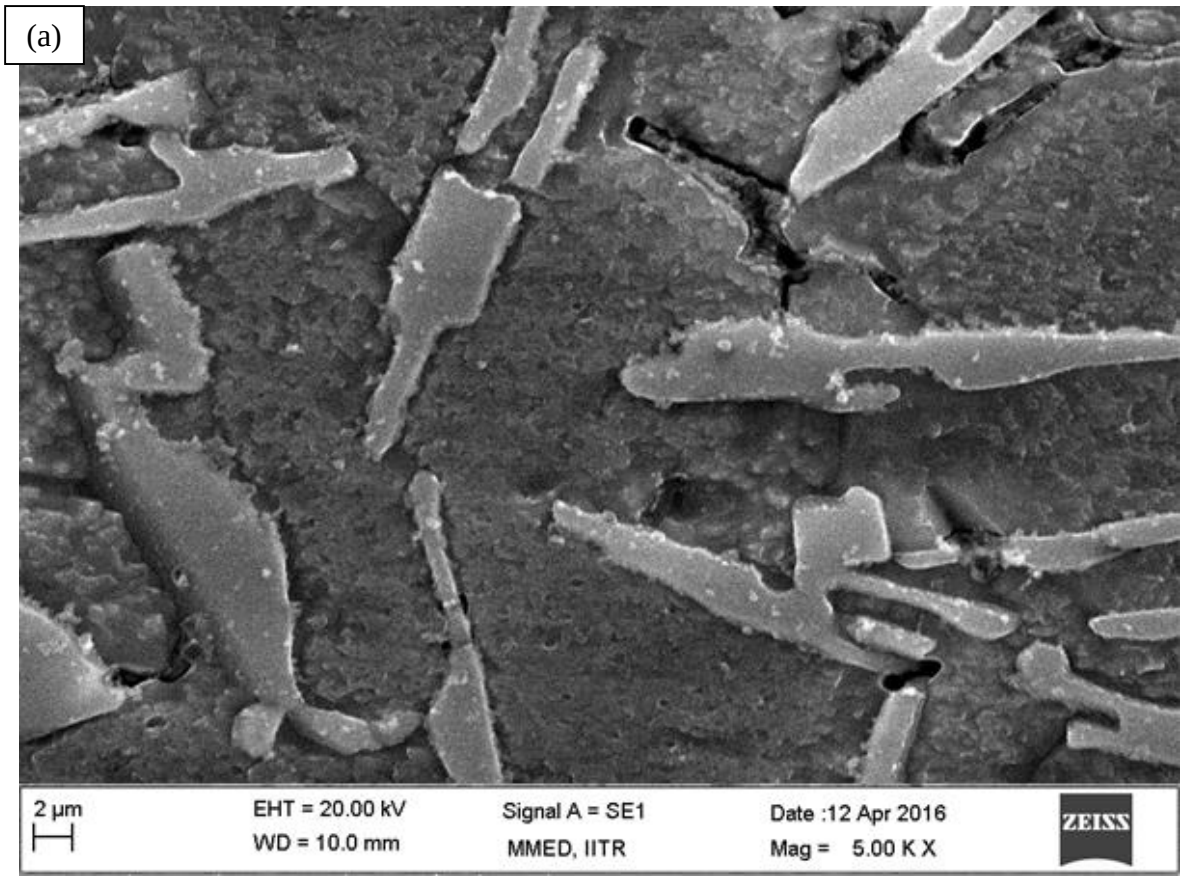

Fig. 5.3 SEM micrograph of Al-12Si-5Gr (a) Spray Formed (b) FSPed

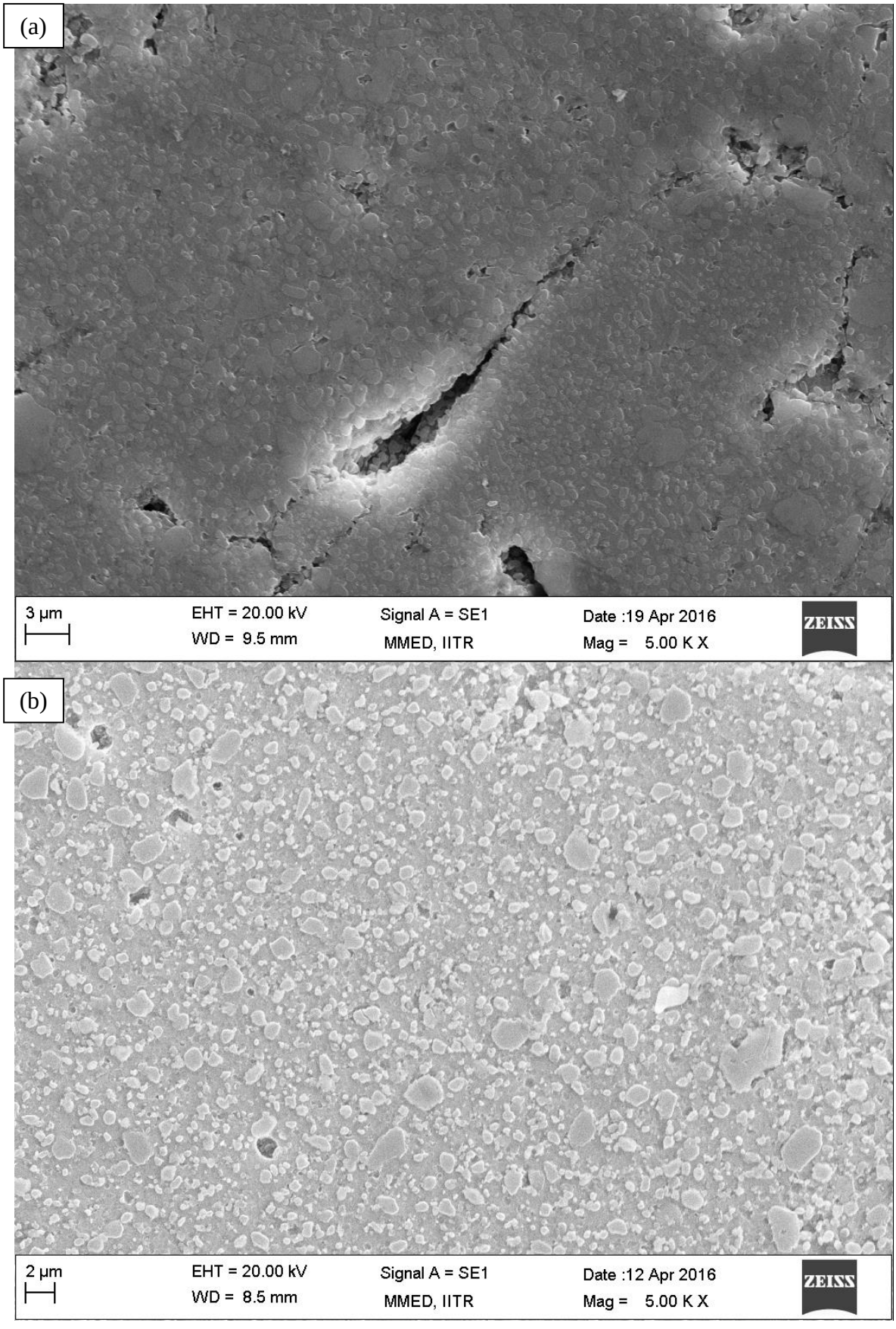

Fig. 5.4 SEM micrograph of Al-18Si-5Gr (a) Spray Formed (b) FSPed

5.3 EDAX ANALYSIS

The phases present in spray deposit is identified by EDAX analysis. The EDAX spectrums of all specimen shows that there is uniform distribution of graphite throughout the sample. Hence, it proves that spray forming is an effective technology to produce Al-Si-Gr composites with uniform distribution of graphite throughout the composite. The white region is Primary silicon phase where as there are some regions where we can easily see eutectic silicon present in the aluminium grains. The black region shows graphite particles. Using mapping technology of EDAX, it was seen that graphite was present on grain boundaries of Al-Si alloy.

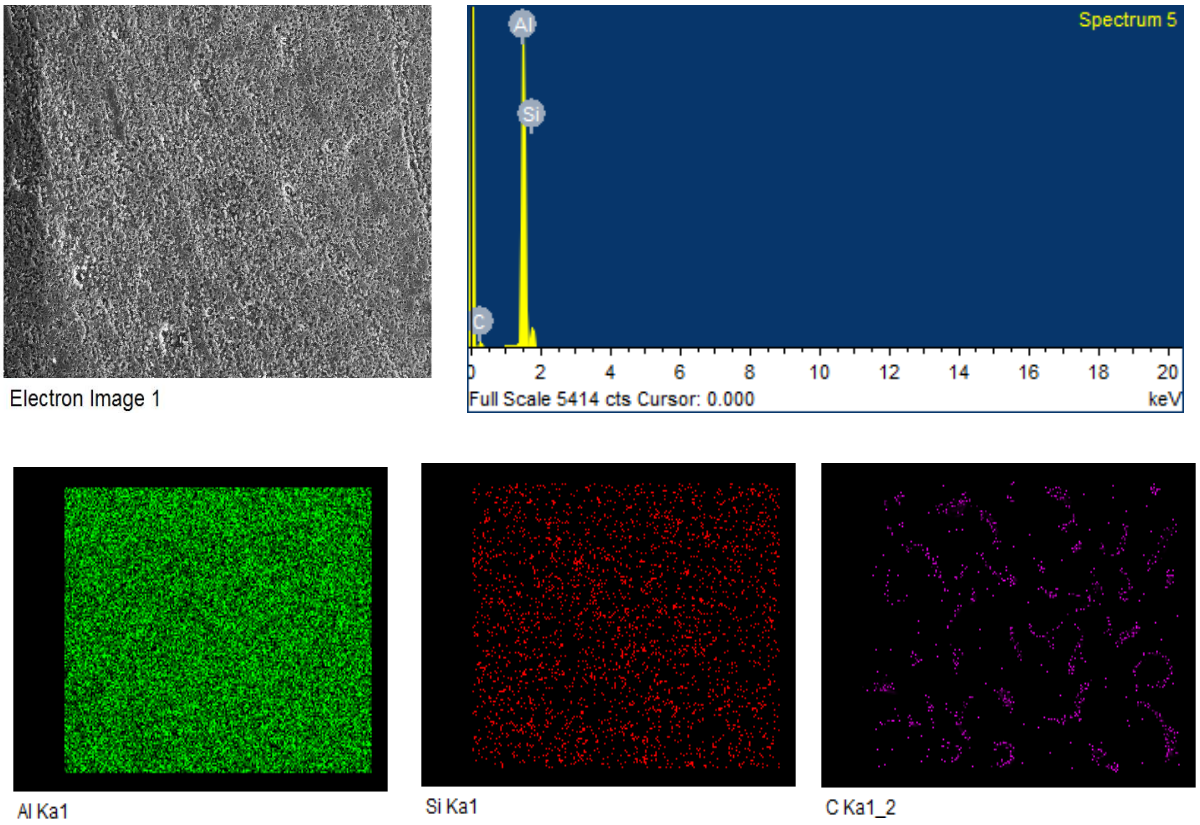

Fig. 5.5 EDAX Spectrum and elemental mapping of Al-6Si-5Gr

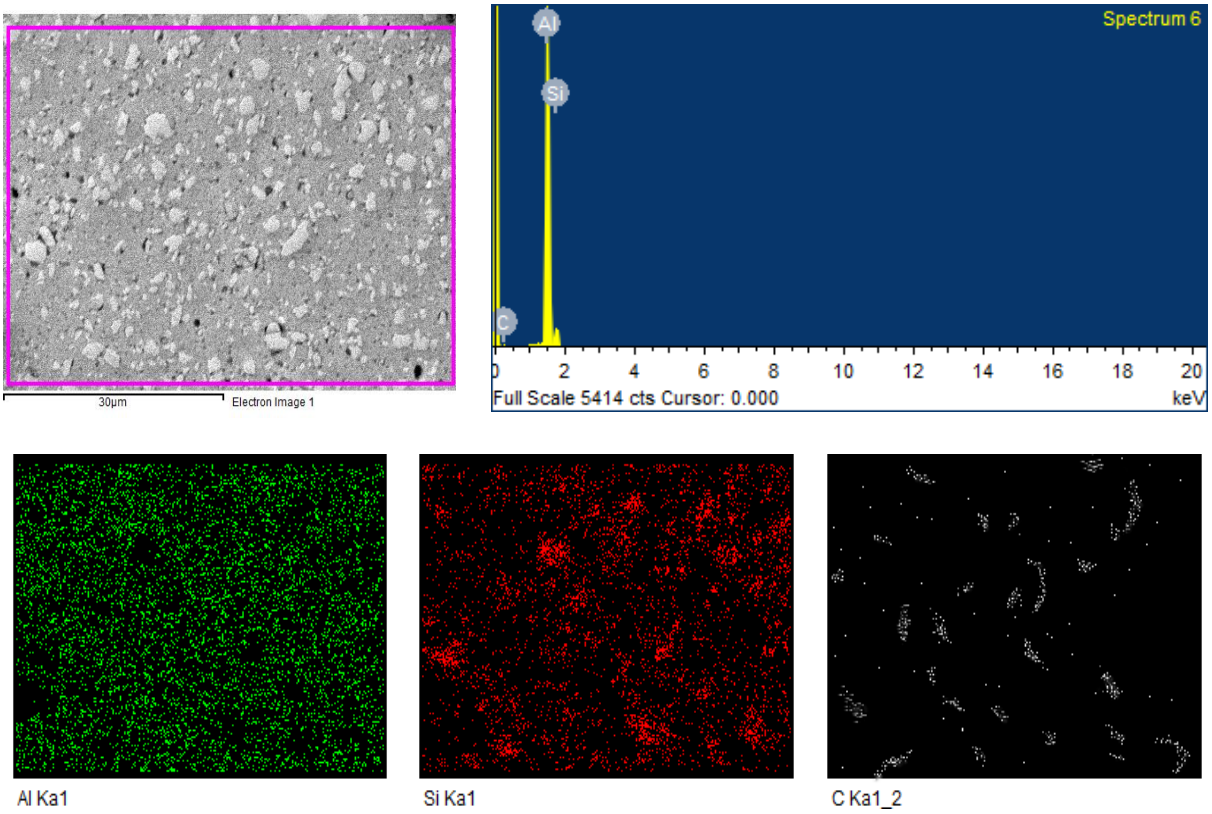

Fig. 5.6 EDAX Spectrum and elemental mapping of Al-12Si-5Gr

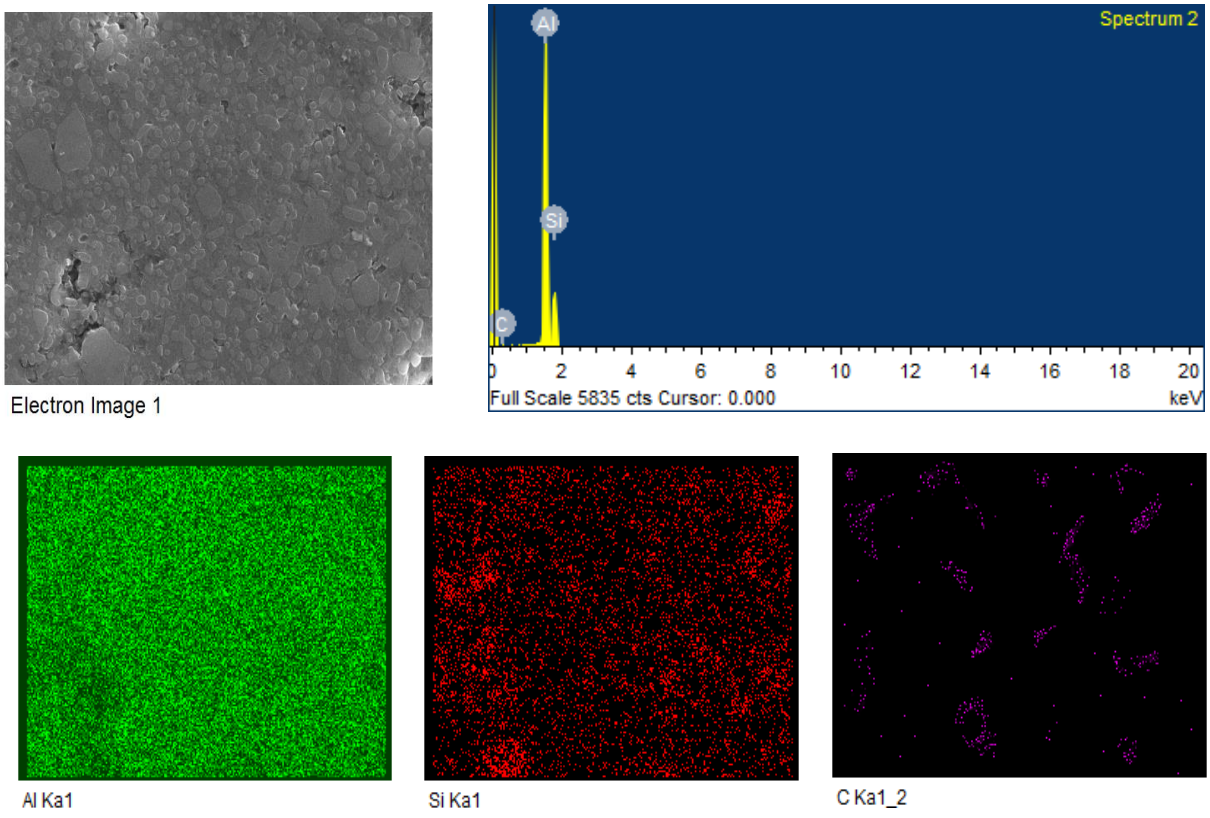

Fig. 5.7 EDAX Spectrum and elemental mapping of Al-18Si-5Gr

5.4 XRD ANALYSIS

Fig. 5.6 shows XRD spectra of spray formed Al-Si-Gr composite before and after FSP. These XRD spectrums clearly shows presence of only three phases in the spray preforms and FSPed samples. XRD of spray formed material shows the presence of graphite in the composite. With the increase in Si content, intensity of peaks of Si in XRD spectra increases. After FSP, XRD spectrum is similar to their spray formed counterparts, this shows absence of any chemical reaction during FSP.

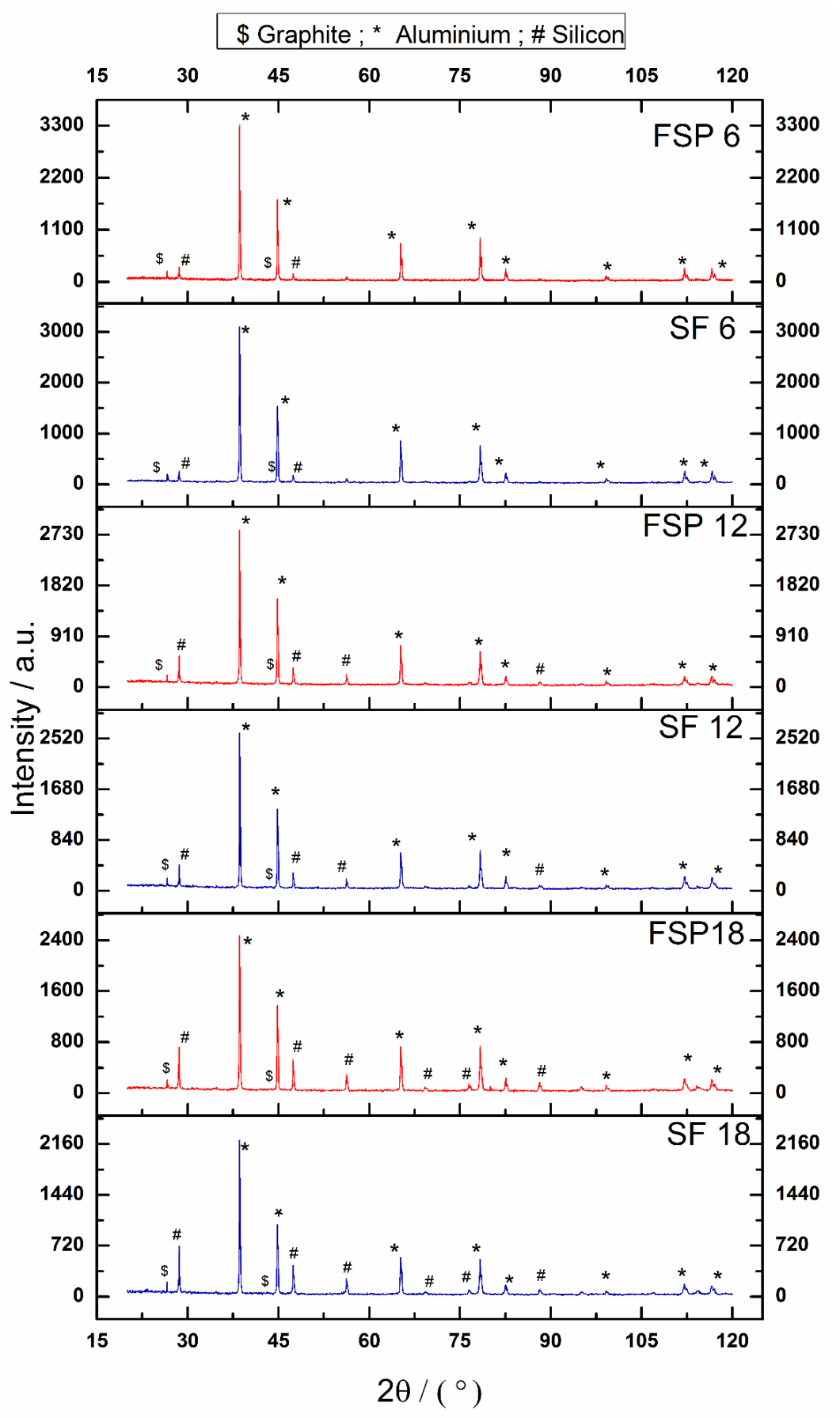

Fig. 5.8 XRD spectra of spray formed Al-Si-Gr composite before and after FSP

5.5 TENSILE STRENGTH

The presence of pores leads to weakening of a material by reducing the amount of stress bearing area and therefore lowers the amount of stress the material is able to withstand. Due to this reason spray formed materials have less strength. Reduction in porosity leads to increase in strength.

Fig. 5.9 shows engineering stress-strain diagrams of all compositions. The diagram clearly shows that there is continuous yielding in all composite compositions. Hence, no yield point can be determined. So, we calculate 0.2% proof stress. Mobile dislocations in aluminium are the reason behind continuous yielding behaviour. The size, shape and distribution of eutectic and primary silicon particles determine the mechanical properties of the Al- Si alloy. Strength properties of Al-Si alloys are enhanced by small, spherical, uniformly distributed silicon particles [2]. Failure of cast aluminium-silicon alloys under a tensile load is caused by cracks initiated from prominent casting defects like porosity. If these defects are minimized or eliminated, the fatigue performance is significantly improved.

Fig. 5.10 shows the increase in ductility and UTS after FSP. Increase in tensile strength after FSP is due to microstructural refinement, elimination of casting defects like porosity and complete homogenization of the microstructure attained after friction stir processing. There is no significant change produced in yield point after FSP. This no significant change in yield strength is produced because of high yield strength of spray formed composite. This high yield strength of Al–Si-Gr composite can be credited to the formation of shallow shrinkage cavity because of enhanced solidification of the molten composite on the spray deposited surface. The yield strength was controlled by the aluminium matrix strength. Aluminium matrix strength depends on the microstructure of the formed composite (i.e., precipitate type and grain size). The increase in ductility after FSP can be attributed to the size reduction of Si phase particles in Al-matrix, complete homogenization of composite and removal of porosity.

Fig. 5.11 shows the changes in stress-strain curves of material with the increase in silicon content. There is increase in UTS, 0.2% proof stress and decrease in ductility with the increase in Si content. Fine dimples present on the cracked surface represents the ductile fracture of all the samples. The decrease in ductility with the increasing amount of silicon may be attributed to the increasing volume fraction of plastically incompatible silicon based phases in the soft and ductile aluminium matrix. There is slight decrease in slope of stress-strain curve

with increase in Si content. This slope represents young's modulus. This shows decrease in modulus of elasticity with increase in Si content. Increasing the Si content results in decrease of the temperature coefficient of modulus of elasticity by increasing covalent contribution to atomic bonding.

Table 5.2 shows the values of UTS, 0.2% Proof stress and ductility at UTS for all compositions. Since there is continuous yielding in our material, so 0.2% proof stress is calculated and then tabulated. The reduced UTS value of Al-18Si-5Gr samples can be primarily credited to the twin effects of the existence of primary silicon and an increase in the porosity and volume fraction of plastically incompatible silicon based phases in the Al-matrix. The presence of plastically incompatible phases (silicon in Al-matrix) leads to the stress accumulation at the interface with the Al-matrix and under uni-axial tensile loading micro voids appear depending on the mechanical properties of the strengthening phase, thus decreasing UTS of the material.

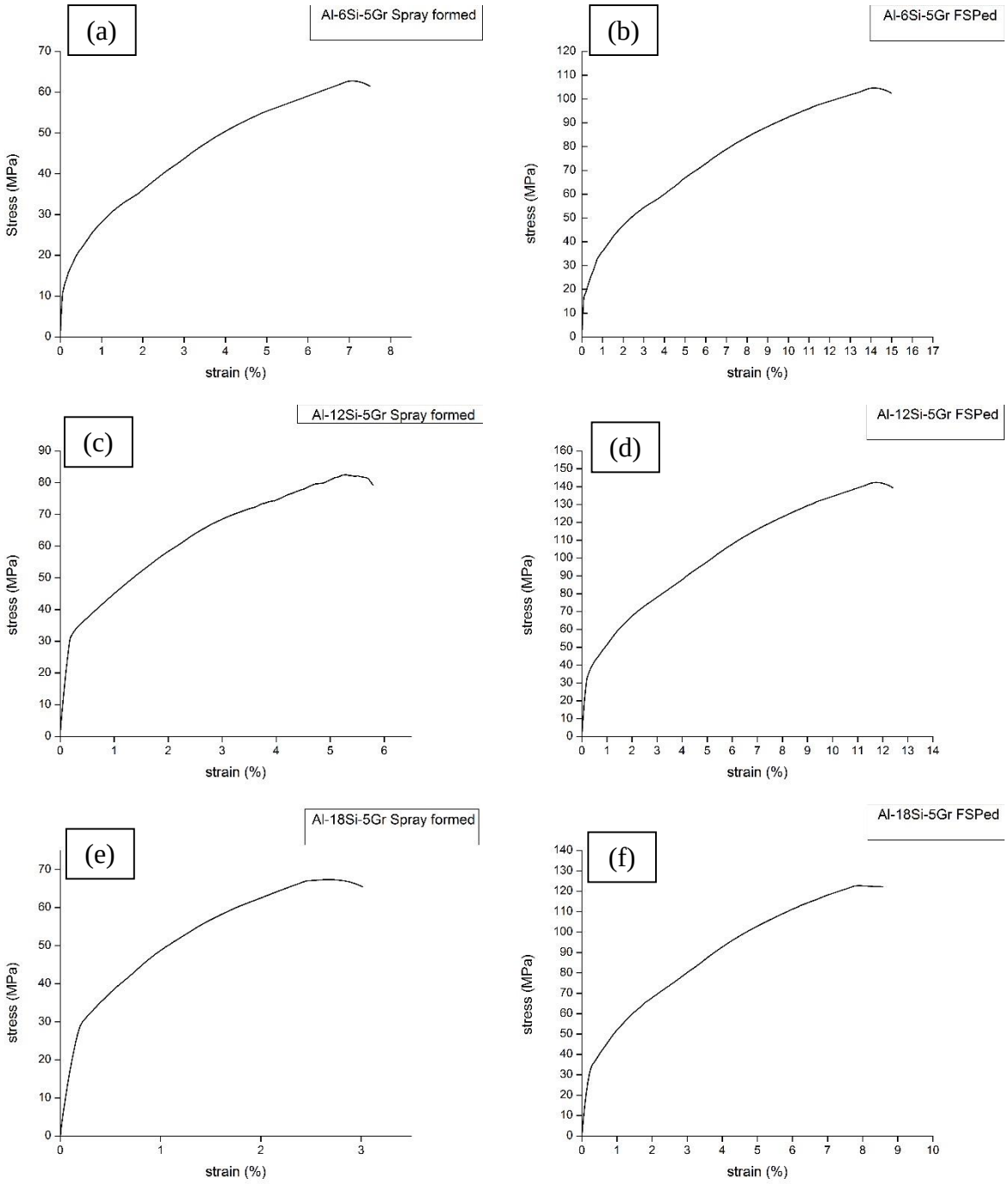

Fig. 5.9 Stress-Strain curves of (a)Al-6Si-5Gr Spray Formed (b) Al-6Si-5Gr FSPed (c) Al-12Si-5Gr Spray Formed (d) Al-12Si-5Gr FSPed (e) Al-18Si-5Gr Spray Formed (f) Al-18Si-5Gr FSPed

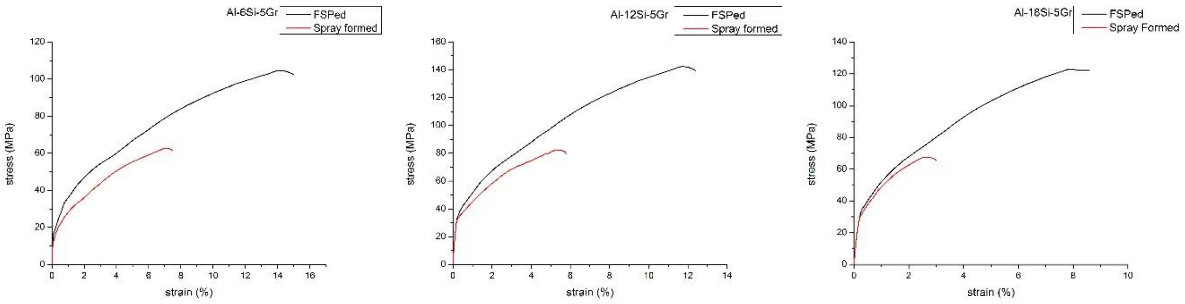

Fig. 5.10 Stress-strain curves of Spray formed materials before and after FSP.

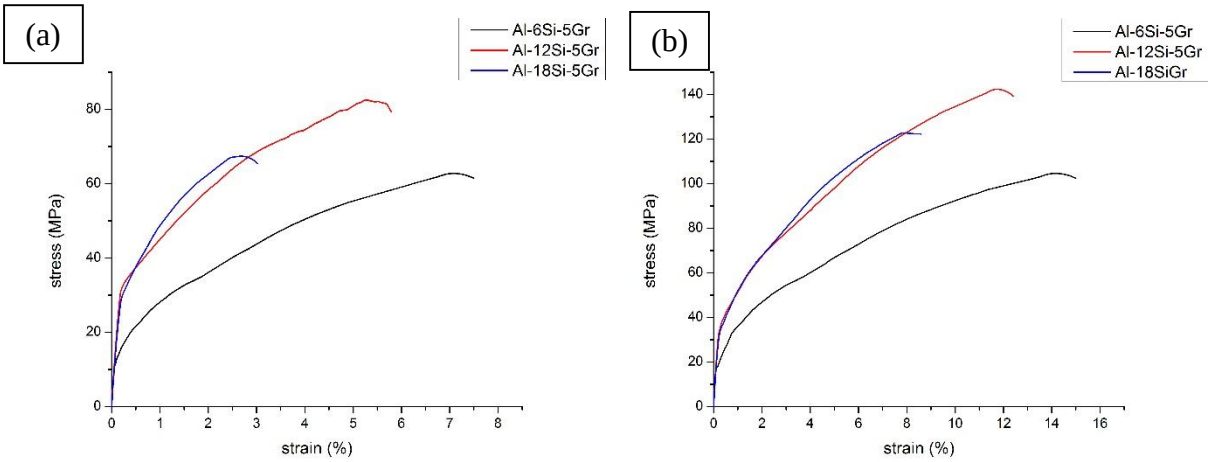

Fig. 5.11 Stress-strain curves (a)Spray formed (b) FSPed

Table 5.2 Tensile test results: UTS, 0.2% proof stress and ductility

Material	Ultimate Tensile Strength (MPa)	0.2% Proof stress(MPa)	Ductility at UTS (%)
Al-18Si-5Gr (Spray formed)	67.42±3.04	39.42±1.32	2.68±0.13
Al-12Si-5Gr (Spray formed)	82.43±4.32	38.04±1.21	5.32±0.38
Al-6Si-5Gr (Spray formed)	62.71±2.78	23.09±1.65	7.14±0.67
Al-18Si-5Gr (Friction stir processed)	123.02±7.61	42.74±2.01	7.82±0.71
Al-12Si-5Gr (Friction stir processed)	142.35±8.82	41.54±2.17	11.71±0.82
Al-6Si-5Gr (Friction stir processed)	104.42±6.67	27.87±1.76	14.01±0.87

5.6 HARDNESS

Table 5.2 shows the calculated hardness values of all the specimens. It can be seen from the table that value of hardness increases with the increase of silicon content. There is a sharp increase in VHN after FSP on spray formed specimens. Fig. 5.10 shows the variation of vicker's hardness with silicon content in both spray formed and FSPed materials.

Hardness of the Al–Si alloy increases with the increase in the silicon content, this increase in hardness is due to the increase of hard silicon phase. Due to intense plastic deformation, recrystallization occurs in stir zone and grain refinement takes place. Grain refinement and reduction in porosity are the major reasons behind the increase of hardness after FSP.

Table 5.3 Hardness value

Specimen	Spray formed	FSPed
Al-6Si-5Gr	41.5±0.7	58.6±1.4
Al-12Si-5Gr	46.3±0.9	66.1±1.5
Al-18Si-5Gr	52.2±1.1	73.9±2.0

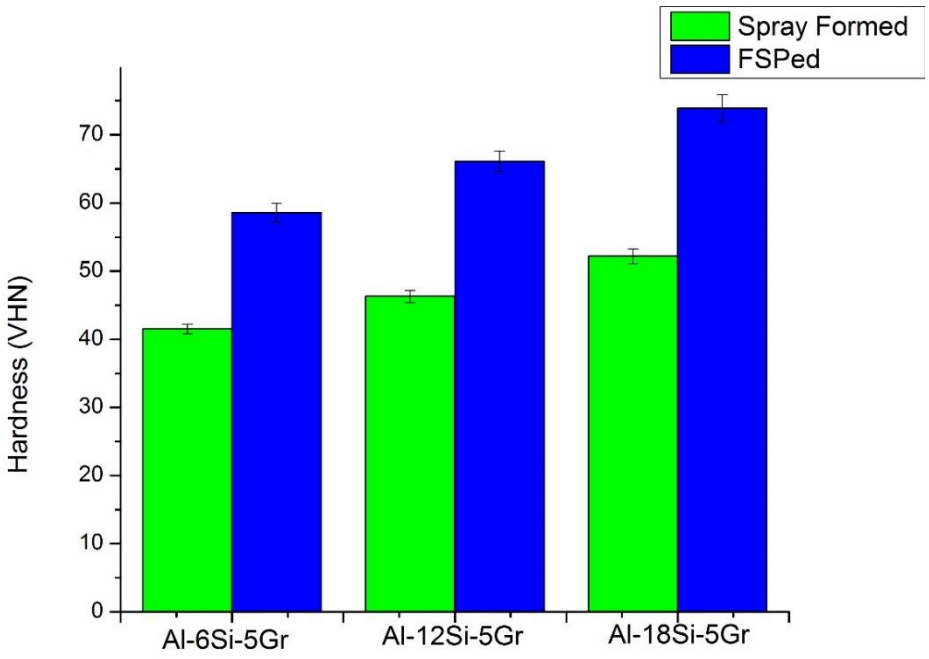

Fig. 5.12 Variation in hardness of spray formed Al-Si-Gr composite before and after FSP

CHAPTER 6
CONCLUSIONS

1. The prepared Al–Si-Gr composites have homogenous distribution of silicon and graphite throughout the spray formed composite. So, spray casting can be used to produce Al-Si-Gr composites.

2. Small grain size of spray formed Al-Si-Gr was further refined by FSP.

3. With the increase of silicon content ductility of the composite is reduced.

4. Al-12Si-5Gr composition has the highest ultimate tensile strength and 0.2% proof stress compared to other two studied compositions.

5. FSP breaks up the coarse Si particles into finer Si particles and distributes them uniformly in the aluminium matrix.

6. FSP results in increased tensile strength, hardness and ductility.

7. With the increase of silicon content hardness increases in Al-Si-Gr composite.

8. FSP reduces the porosity to a great extent. So, FSP can be considered as the suitable secondary processing after FSP to remove defects produced during spray forming.

9. FSP offers very attractive possibilities for commercial success. FSP improves the overall performance of the spray-formed Aluminium silicon graphite composite.

CHAPTER 7
SCOPE FOR FUTURE WORK

1. Spray forming can be used to produce composites of different compositions. This process can be easily used to increase graphite content or add other alloying elements like iron, nickel etc. in composite. So as to have less wear rate and coefficient of friction, composites of different compositions can be easily produced. In future composites of better compositions can be produced with better mechanical properties.

2. FSP can be easily used in all aluminium based spray formed material. So, this process can be effectively used in future to eliminate porosity from spray deposited material. So, FSP in spray formed material is a better secondary processing than old rolling, extrusion and forging techniques.

3. Different processing parameters like rotating speed and traverse speed can be used to get better results. Increasing number of passes of FSP on spray formed material can be used for further grain refinement and improved mechanical properties.

CHAPTER 8
REFERENCES

[1] R. K. Endo, Y. Fujihara and M. Susa, 'Calculation of Density and Heat Capacity of Silicon by Molecular Dynamics Simulation', High Temperatures-High Pressures, 36.5 (2003), pp. 505-511.

[2] B. Mathai and others, 'Effect of Silicon on Microstructure and Mechanical Properties of Al-Si Piston Alloys', International Journal of Engineering Trends and Technology, 29.6 (2015), pp. 299–303.

[3] J. Martin, 'Micro mechanisms in particle hardened aslloys',3rd Ed., Cambridge University Press, Cambridge, (1980), pp.60.

[4] Q. Zhang, B.L. Xiao, W.G. Wang, Z.Y. Ma, 'Reactive mechanism and mechanical properties of in situ composites fabricated from an Al–TiO system by friction stir processing', Acta Materialia 60 (2012), pp. 7090–7103.

[5] N. Hansen, 'Hall-Petch Relation and Boundary Strengthening', Scripta Materialia, 51.8 (2004), pp. 801–806 .

[6] R. Mittal and D. Singh, 'Dry Sliding Wear Behavior of Cold Rolled Spray Cast Al-6Si Alloy', Transactions of the Indian Institute of Metals, 67.4 (2014), pp. 551–557.

[7] A. S., Srivatsan S., W. Yue and E.J. Lavernia, 'Processing, microstructure and fracture behaviour of a spray atomized and deposited Al-Si alloy', Journal of Material Science, 32(1997), pp. 2835-2848.

[8] V.C. Srivastava, R.K. Mandal and S.N. Ojha, 'Microstructure and Mechanical Properties of Al–Si Alloys Produced by Spray Forming Process', Materials Science and Engineering: A, 304-306 (2001), pp. 555–558.

[9] R. P. Underhill, P. S. Grant and B. Cantor, 'Microstructure of Spray-Formed AI Alloy', Materials & Design, 14.1 (1993), pp. 45–47.

[10] M. W. Mahoney and others, 'Properties of Friction-Stir-Welded 7075 T651 Aluminum', Metallurgical and Materials Transactions A, 29.7 (1998), pp.1955–1964 .

[11] P. S. Grant, 'Spray Forming', Progress in Materials Science, 39.95 (1995), pp. 497–545 .

[12] K. V. Ojha and others, ‘Shape, Microstructure and Wear of Spray Formed Hypoeutectic Al-Si Alloys’, Materials Science and Engineering A, 487.1-2 (2008), pp. 591–596 .

[13] K. K. Sahu, R. K. Dube and S. C. Koria, ‘Aspects of Porosity Formation in Spray Deposited Thin Aluminium Strip’, Powder Metallurgy, 52.2 (2009), pp. 135–144.

[14] W.D. Cai and E.J. Lavernia, ‘Modeling of Porosity during Spray Forming’, Materials Science and Engineering A, 29B (1997), pp. 8–12.

[15] R. M. Ward and others, ‘A Simple Transient Numerical Model for Heat Transfer and Shape Evolution during the Production of Rings by Centrifugal Spray Deposition’, journal of materials science, 39.9 (2004), pp.7259–7267.

[16] W. Cai and E. J. Lavernia, ‘Modeling of Porosity during Spray Forming: Part I. Effects of Processing Parameters’, Metallurgical and Materials Transactions B, 29B (1998), pp. 1085–1096.

[17] B. P. Bewlay and B. Cantor, ‘Gas Velocity Measurements from a Close-coupled Spray Deposition Atomizer’, Material Science and Engineering A, 8 (1989), pp. 207–222.

[18] C. Cui, F. Cao and Q. Li, ‘Formation Mechanism of the Pressure Zone at the Tip of the Melt Delivery Tube during the Spray Forming Process’, Journal of Materials Processing Technology, 137.1-3 (2003), pp. 5–9.

[19] B. Cantor, K.H. Baik and P.S. Grant, ‘Development of Microstructure in Spray Formed Alloys’, Progress in Materials Science, 42.1-4 (1997), pp.373–392.

[20] V. C. Srivastava and others, ‘Microstructural Modifications Induced during Spray Deposition of Al-Si-Fe Alloys and Their Mechanical Properties’, Materials Science and Engineering A, 471.1-2 (2007), pp. 38–49.

[21] C. Suryanarayana, ‘Non-equilibrium Processing of Materials’ ISBN: 978-0-08-042697-6 Pergamon Materials Series, 2 (1999), pp. 427-438.

[22] P. Mathur and others, ‘Spray Casting: An Integral Model for Process Understanding and Control’, Materials Science and Engineering: A, 142.1-2 (1991),pp. 261–276.

[23] B. J. Hamrock, S. R. Schmid, B. O. Jacobson, ‘Fundamentals of Fluid Film Lubrication’ second edition marcel dekker inc. New York basel (2005), pp. 251-280.

[24] M. Gupta and S. Ling, ‘Microstructure and Mechanical Properties of Hypo/hyper-Eutectic Al-Si Alloys Synthesized Using a near-Net Shape Forming Technique’, Journal of Alloys and Compounds, 287.1-2 (1999), pp. 284–294.

[25] F. Wang and others, ‘Effect of Si Content on the Dry Sliding Wear Properties of Spray-Deposited Al–Si Alloy’, Materials & Design, 25.2 (2004), pp. 163–166.

[26] R. Cobden and A. Banbury, ‘Aluminium: Physical Properties, Characteristics and Alloys’, Talal Lecture 1501, (1994), pp.60.

[27] M. M. Dave, K. D. Kothari, ‘Composite Material-Aluminium Silicon Alloy : A Review’, ISSN - 2250-1991Research paper engineering, 2.3 (2013), pp. 2009–2011.

[28] Dr A. Lambourne, ‘Spray forming of Si-Al alloys for Thermal management applications’ D.Phil. Thesis, (2007), Queens College.

[29] ASM International, ‘Introduction to Aluminum-Silicon Casting Alloys’, Aluminum-Silicon Casting Alloys Atlas of Microfractographs, 2 (2004), pp. 1–10.

[30] D. Hull, T. Clyne, ‘An introduction to composite materials’, 2nd edition, Cambridge university press (1996), pp.66.

[31] G. Liu and others, ‘Microstructural Aspects of the Friction-Stir Welding of 6061-T6 Aluminum’, Scripta Materialia, 37.3 (1997), pp.355–361.

[32] Y. J. Kwon, I. Shigematsu and N. Saito, ‘Mechanical Properties of Fine-Grained Aluminum Alloy Produced by Friction Stir Process’, Scripta Materialia, 49.8 (2003), pp.785–789.

[33] Y. S. Sato and others, ‘Microstructural Evolution of 6063 Aluminum during Friction-Stir Welding’, Metallurgical and Materials Transactions A, 30.9 (1999), pp. 2429–2437.

[34] B. Heinz and B. Skrotzki, ‘Characterization of a Friction-Stir-Welded Aluminum Alloy 6013’, Metallurgical and Materials Transactions B, 33.3 (2002), pp. 489–498.

[35] R.S. Mishra and Z.Y. Ma, ‘Friction Stir Welding and Processing’, Materials Science and Engineering: R: Reports, 50.1-2 (2005), pp. 1–78.

[36] W.M. Thomas, E.D. Nicholas, J.C. Needham, M.G. Murch, P. Templesmith, C.J. Dawes G.B. Patent application no. 9125978.8, December 1991.

[37] C. Dawes, W. Thomas, TWI Bulletin 6, November/December 1995, pp. 124.

[38] R. S. Mishra, M. W. Mahoney, ‘Friction Stir Processing: A New Grain Refinement Technique to Achieve High Strain Rate Superplasticity in Commercial Alloys’, Materials Science Forum, 35.7 (2001), pp. 357-359.

[39] R. S. Mishra and others, ‘High Strain Rate Superplasticity in a Friction Stir Processed 7075 Al Alloy’, Scripta Materialia, 42.2 (1999), pp. 163–168.

[40] L. Karthikeyan, V. S. Senthilkumar and K. A. Padmanabhan, ‘On the Role of Process Variables in the Friction Stir Processing of Cast Aluminum A319 Alloy’, Materials and Design, 31.2 (2010), pp. 761–771.

[41] Z. Y. Ma, S. R. Sharma and R. S. Mishra, ‘Effect of Friction Stir Processing on the Microstructure of Cast A356 Aluminum’, Materials Science and Engineering A, 433.1-2 (2006), pp. 269–278.

[42] J. Gandra, R. M. Miranda and P. Vilaça, ‘Effect of Overlapping Direction in Multipass Friction Stir Processing’, Materials Science and Engineering A, 528.16-17 (2011), pp.5592–5599.

[43] A. G. Rao and others, ‘Microstructural Refinement of a Cast Hypereutectic Al-30Si Alloy by Friction Stir Processing’ ,Materials Letters, 63.30 (2009), pp. 2628–2630.

[44] F. Y. Tsai and P. W. Kao, ‘Improvement of Mechanical Properties of a Cast Al-Si Base Alloy by Friction Stir Processing’ ,Materials Letters, 80 (2012), pp. 40–42.

[45] M. L. Santella and others, ‘Effects of Friction Stir Processing on Mechanical Properties of the Cast Aluminum Alloys A319 and A356’ ,Scripta Materialia,53.2 (2005), pp. 201–206.

[46] T. S. Mahmoud, ‘Surface Modification of A390 Hypereutectic Al-Si Cast Alloys Using Friction Stir Processing’, Surface and Coatings Technology, 228 (2013), pp. 209–220.

[47] L. Karthikeyan and others, ‘Mechanical Property and Microstructural Changes during Friction Stir Processing of Cast Aluminum 2285 Alloy’, Materials and Design, 30.6 (2009), pp. 2237–2242.

[48] R. Kapoor and others, ‘Effect of Friction Stir Processing on the Tensile and Fatigue Behavior of a Cast A206 Alloy’, Materials Science and Engineering A, 561 (2013), pp.159–166.

[49] R. P. Underhill, P. S. Grant and B. Cantor, ‘Microstructure of spray-formed AI alloy 2618’, Materials & Design,14.1 (1993) pp. 45-47.